Review of Heat Conduction in Nanofluids

Jing Fan

Liqiu Wang[1]
e-mail: lqwang@hku.hk

Department of Mechanical Engineering,
University of Hong Kong,
Pokfulam Road,
Hong Kong

Nanofluids—fluid suspensions of nanometer-sized particles—are a very important area of emerging technology and are playing an increasingly important role in the continuing advances of nanotechnology and biotechnology worldwide. They have enormously exciting potential applications and may revolutionize the field of heat transfer. This review is on the advances in our understanding of heat-conduction process in nanofluids. The emphasis centers on the thermal conductivity of nanofluids: its experimental data, proposed mechanisms responsible for its enhancement, and its predicting models. A relatively intensified effort has been made on determining thermal conductivity of nanofluids from experiments. While the detailed microstructure-conductivity relationship is still unknown, the data from these experiments have enabled some trends to be identified. Suggested microscopic reasons for the experimental finding of significant conductivity enhancement include the nanoparticle Brownian motion, the Brownian-motion-induced convection, the liquid layering at the liquid-particle interface, and the nanoparticle cluster/aggregate. Although there is a lack of agreement regarding the role of the first three effects, the last effect is generally accepted to be responsible for the reported conductivity enhancement. The available models of predicting conductivity of nanofluids all involve some empirical parameters that negate their predicting ability and application. The recently developed first-principles theory of thermal waves offers not only a macroscopic reason for experimental observations but also a model governing the microstructure-conductivity relationship without involving any empirical parameter.
[DOI: 10.1115/1.4002633]

Keywords: nanofluids, heat conduction, experiments, models, dual-phase-lagging, thermal wave

1 Introduction

The low thermal conductivities of conventional heat transfer fluids limit their cooling performance in many industrial applications and thus inspired intensive research efforts to resolve this problem. It has been known for long time since Maxwell published his theoretical work of predicting the thermal conductivity of mixtures in the 19th century [1,2] that the fluid thermal conductivity can be increased by suspending some higher-conductivity substances such as solid particles. However, the suspensions with millimeter- or micrometer-sized particles cannot be applied in many microcooling devices due to issues of the possible sedimentation, clogging, erosion, and excessive pumping-power requirement. The modern nanotechnology makes the generation of nanosized particles possible, thus offering an ideal candidate for replacing microsized particles in upgrading fluid conductivity. The concept of "nanofluids" was first proposed by Choi et al. [3] as a new class of heat transfer fluids engineered by suspending some metallic nanoparticles in ordinary fluids to boast fluid conductivity. Since then, nanofluids have attracted intensive interest which expands the scope into nanofluids engineered by suspending other nanostructures such as oxide nanoparticles, nanofibers, carbon nanotubes, and even nanodroplets [4–11]. Figure 1 shows transmission electron microscopy (TEM) or scanning electron microscope (SEM) images of some nanoparticles or nanotubes used in nanofluids, illustrating the wide range of nanostructures proposed for nanofluids. Readers are referred to Refs. [5,14–16] for the approaches for synthesizing nanofluids of various microstructures.

Research on heat conduction in nanofluids ranges from conductivity measurement to extension of existing models and development of new models for conductivity prediction. However, there is still a lack of agreement either among experiments or among theories. The present work reviews advances in our understanding of heat conduction in nanofluids. Section 2 centers on experimental findings, including conductivity measurements and its features. Section 3 is on heat-conduction mechanisms in nanofluids. Section 4 details theoretical models of both conventional and newly developed types for predicting nanofluids thermal conductivity. Some concluding remarks are drawn in Sec. 5.

2 Experimental Findings

2.1 Thermal Conductivity. As a standard transient technique, the hot-wire method is widely used to measure the thermal conductivity of nanofluids because of its easy and fast operation and its high accuracy [5]. In this method, a thin metallic wire (hot wire, ideally with infinite thermal conductivity and zero heat capacity) is embedded in the test liquid as both the heat source and the temperature sensor. The thermal conductivity of the test sample can be derived from the temperature change of the hot wire over a specific time interval. The relation between the two is normally developed based on assumptions that the hot wire is a line heat source of infinite thin and infinite long and the fluid is homogeneous, isotropic and with infinite amount and constant initial temperature [17]. The measurement usually lasts for only several seconds so that the effect of natural convection can be neglected. The details of this method are available in Refs. [5,17,18]. The modification of the conventional single-wire hot-wire method is also made in Ref. [19] by using two wires with different lengths to reduce the end effect. The other techniques for conductivity measurement include the temperature oscillation method [20], the thermal comparator method [21], and the steady-state parallel-

[1]Corresponding author.

Contributed by the Heat Transfer Division of ASME for publication in the JOURNAL OF HEAT TRANSFER. Manuscript received December 31, 2009; final manuscript received September 24, 2010; published online January 10, 2011. Editor Yogesh Jaluria.

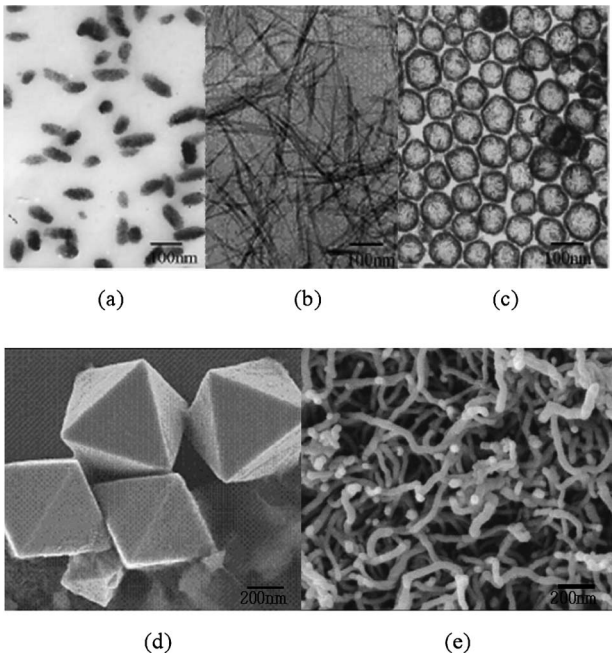

Fig. 1 TEM/SEM pictures of nanoparticles/nanotubes from "drying" samples of nanofluids [10,12,13]: (*a*) elliptical Cu nanoparticles, (*b*) $CePO_4$ nanofibers, (*c*) hollow CuS nanoparticles, (*d*) octahedral Cu_2O nanoparticles, and (*e*) carbon nanotubes

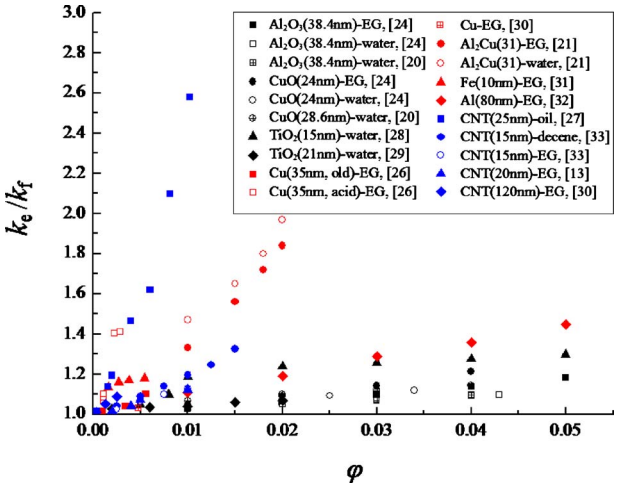

Fig. 2 Comparison of experimental data on effective thermal conductivity of nanofluids

plate method [22].

Thermal conductivity measurements for nanofluids started with oxide nanoparticle suspensions. Masuda et al. [23] experimentally showed in 1993 that the thermal conductivity of water can be increased by 30% after suspending ultrafine alumina (Al_2O_3) particles (13 nm in the mean diameter) in it at a volume fraction of 4.3%. Later in 1999, Lee et al. [24] produced Al_2O_3 and copper oxide (CuO) nanofluids with water and ethylene glycol (EG) as the base fluids and measured their thermal conductivity by using the transient hot-wire method. It was found that the thermal conductivity of both nanofluids increases linearly with the particle volume fraction. The measured conductivity in Ref. [24] is slightly lower but much higher than Hamilton–Crosser predictions for Al_2O_3 and CuO nanofluids, respectively. However, the significant difference between the two for CuO nanofluids may come from the extremely small value of CuO conductivity used in the Hamilton–Crosser prediction [25]. The nanoparticle size was proposed to be responsible for the difference because the average sizes of used Al_2O_3 and CuO particles are 38 nm and 24 nm, respectively.

Nanofluids had not received much attention until Eastman et al. [26] reported in 2001 their experiments of a substantially higher conductivity of copper (Cu)-EG nanofluids than that for the pure ethylene glycol or oxide-EG nanofluids at the same particle volume fraction. The one-step method was used to disperse Cu nanoparticles of average diameter less than 10 nm into ethylene glycol in Ref. [26]. With less than 1% thioglycolic acid as the stabilizer, 0.3 vol % of such particles gives rise to an increase in thermal conductivity of ethylene glycol by 40% [26]. Without the stabilizer, the thermal conductivity of the Cu-EG nanofluids with the same particle volume fraction is lower [26]. The conductivity enhancement of such metallic nanofluids reported in Ref. [26] is much more significant than that of the oxide nanofluids reported earlier.

Choi et al. [27] made an attempt to disperse multiwalled carbon nanotubes (MWCNTs) into oil and measure its conductivity. Up to 160% enhancement of thermal conductivity was observed at a nanotube volume fraction of only 1%. The organized liquid molecular structure at the solid-liquid interface was suggested to be the reason for the energy transport enhancement between the two phases. They also observed a nonlinear relationship between the thermal conductivity enhancements and the nanotube loading, a phenomenon also found in oxide and metallic nanofluids.

Figure 2 shows the measured conductivity ratio k_e/k_f at the room temperature as a function of the particle volume fraction φ for oxide, metallic, and CNT nanofluids. Here k_e and k_f are the nanofluid effective thermal conductivity and the base fluid conductivity, respectively. The conductivity enhancement of oxide nanofluids is usually less than that of the other two types of nanofluids. Both metallic particles and CNTs may generate a very significant conductivity enhancement. There exists a wide scattering of experimental data (Fig. 2).

Although the Al_2O_3/CuO/Cu/CNTs-water/EG combinations are still popular, some other particle-fluid combinations have been attempted. The thermal conductivity of silicon carbide (SiC)-water/EG nanofluids was measured in Ref. [34], showing up to 15.8% conductivity increase at a volume fraction of 4.2% for spherical SiC particles and up to 22.9% at a volume fraction of 4% for cylinder SiC particles. However, no significant conductivity enhancement was observed for nanofluids of C_{60}–C_{70} fullerene nanoparticles in toluene ($<1\%$ for particle volume fractions less than 0.6%) and gold (Au) in ethanol (the largest increase is $1.3\% \pm 0.8\%$ for Au volume fractions less than 0.6%) [35]. Wang et al. [10] emulsified olive oil into distilled water with small amount of cetyltrimethyl ammonium bromide (CTAB) under ultrasonic disruption. An extraordinary conductivity enhancement (up to 153% at the oil volume fraction of 3.3%) was obtained although the thermal conductivity of olive oil is much smaller than water conductivity. This phenomenon was believed to be an evidence of the presence of thermal waves in nanofluids [10] and was further confirmed by the extraordinarily high thermal conductivity of corn-oil-in-water emulsion [11].

Table 1 summarizes experimental data of thermal conductivity of various nanofluids at the room temperature. There exist wide discrepancies and inconsistencies in these data so that more in-depth research is in demand on heat conduction in nanofluids. The recent first-principles model shows that the presence of nanoparticles leads to a dual-phase-lagging heat conduction in nanofluids at the macroscale rather than the *postulated* Fourier heat conduction [10,16]. The thermal conductivity data available in the literature are, however, obtained based on Fourier law of heat conduction and thus not the intrinsic thermal conductivity of the nanofluids. They should be reviewed as some kind of apparent

Table 1 Summary of experimental data on nanofluid thermal conductivity (MWCNT: multiwalled carbon nanotube; SWCNT: single-walled carbon nanotube; NT: nanotube; EG: ethylene glycol; DE: decene; EO: engine oil; D: diameter; L: length)

Investigator	Particles	Base fluids	Particle size (nm)	Thermal conductivity enhancement
Lee et al. [24]	Al_2O_3	Water/EG	38.4	9%/18% increase for 4.3 vol % Al_2O_3-water/5 vol % Al_2O_3-EG
Lee et al. [36]	Al_2O_3	Water	30 ± 5	1.44% increase at 0.3 vol %
Masuda et al. [23]	Al_2O_3	Water	13	30% increase at 4.3 vol %
Wang et al. [37]	Al_2O_3	EG	28	40% increase for 8 vol % Al_2O_3-EG
Das et al. [20]	CuO	Water	28.6	13% increase at 4 vol %
Masuda et al. [23]	CuO	Water/EG	24	11%/20% increase for 3.4 vol % CuO-water /4 vol % CuO-EG
Wang et al. [22]	CuO	water/EG	23	30% /50% increase for 10 vol% CuO-water /15 vol% CuO-EG
Wei et al. [12]	Copper oxide (Cu_2O)	Water	200	17% decrease to 24% increase (30°C)
Duangthongsuk et al. [29]	Titania (TiO_2)	Water	21	7% increase at 2 vol %
Murshed et al. [28]	TiO_2	Water	15(sphere)/10(cylinder)	Up to 30%/32.8% increase for 5 vol % sphere /5 vol % cylinder
Xie et al. [34]	SiC	Water/EG	26(sphere)/600(cylinder)	15.8% /22.9% increase for 4.2 vol % sphere /4 vol % cylinder
Assael et al. [30]	Cu	EG	120	3% increase at 0.48 vol %
Eastman et al. [26]	Cu	EG	<10	Up to 40% increase at 0.3 vol %
Murshed et al. [32]	Aluminum (Al)	EG	80	>40% increase at 5 vol %
Chopkar et al. [21]	Al_2Cu/Ag_2Al	Water	30–40/30	100% increase at 2 vol-%
Patel et al. [18]	Silver (Ag)	Citrate	10–20	3% increase at 0.001 vol %
Hong et al. [31,37]	Iron (Fe)	EG	10	up to 18% increase at 0.55%
Patel et al. [18]	Au	Thiolate/citrate	3–4/10–20	6%/4.5% increase for 0.011 vol % Au-thiolate/0.00026 vol % Au-citrate
Putnam et al. [35]	Au	Ethanol	4	1.3 ± 0.8% increase at <0.6 vol %
Zhang et al. [38]	Au	Toluene	1.65	Little change, increase or decrease
Assael et al. [39,40]	MWCNT	Water	D15–130, L50 μm	Up to 38% increase at 0.6 vol %
Choi et al. [27]	MWCNT	Oil	D25, L50 μm	up to 160% increase at 1 vol %
Ding et al. [41]	MWCNT	Water	D20–30, L: tens of μm	Up to 27% increase at 1 wt%
Liu et al. [13]	MWCNT	EG/EO	D20–30	12.4% /30% increase for 1 vol % EG /2 vol % EO
Xie et al. [33]	MWCNT	Water/EG/DE	D15, L30 μm	7%/13%/19% increase for 1 vol % CNT-water/EG/DE
Biercuk et al. [42]	SWCNT	Epoxy	D3–30	Up to 125% increase at 1 wt %
Chen et al. [43]	Titanate NT	Water	D10, L100	<4% increase at 0.6 vol %
Putnam et al. [35]	Fullerene	Toluene	-	<1% increase at <1 vol %
Wang et al. [10]	Cerium orthophosphate ($CePO_4$)	Water	$D<10$, L200–300	3.3% decease to 12.9% increase
Putnam et al. [35]	Water	Ethanol	-	6% increase at 2 vol %
Wang et al. [10]	Olive oil	Water	192	Up to153% increase at 3.3 vol %

thermal conductivity k_a that is related to the intrinsic thermal conductivity k by $k_a=k(1-q^2/\rho^2C^3T^3)$ [44]. Here ρ, C, T, and q are the nanofluid density, the specific heat, the temperature, and the heat flux, respectively. Therefore, the apparent thermal conductivity extracted from experimental data assuming Fourier heat conduction is a function of heat flux and is always smaller than the intrinsic thermal conductivity [44].

2.2 Parameter Effects. A relatively intensified effort has been made on revealing the effects of different parameters on the thermal conductivity enhancement of nanofluids through some systematic experiments. Although there is still no consensus on the effects of some parameters, the data from these experiments have enabled some trends to be identified. For oxide and metallic nanofluids, all early experiments showed a linear relationship between the thermal conductivity ratio k_e/k_f and the particle volume fraction φ until the experiment on TiO_2-water nanofluids conducted by Murshed et al. [28]. They dispersed TiO_2 nanoparticles of both rod-shape (diameter of 10 nm by length of 40 nm) and spherical shape (diameter of 15 nm) into de-ionized water and found a nonlinear relationship between k_e/k_f and φ for both cases. The increase of k_e/k_f with φ is more sharp when φ is small. The nonlinearity of $k_e/k_f\sim\varphi$ relation was also observed in several following experiments such as for Al_2O_3-water nanofluids [40,45], Fe-EG nanofluids [37], Al_2Cu/Ag_2Al-water nanofluids [21], and nanotube suspensions [27,41,46]. The measurements by Wang et al. [10] on $CePO_4$-water nanofluids and Wei et al. [12] on Cu_2O-water nanofluids even showed that the thermal conductivity ratio k_e/k_f not necessarily increases with particle volume fraction.

Das et al. [20] first studied the temperature effect on thermal conductivity enhancement in nanofluids. Their measurements indicated a two- to fourfold increase of thermal conductivity ratio k_e/k_f in Al_2O_3/CuO-water nanofluids over a temperature range from 20°C to 50°C. The motion of nanoparticles was suggested to be responsible for the observed strong sensitivity to the temperature. For the MWCNT-water nanofluids, the temperature effect identified in Ref. [46] showed an almost linear increase of k_e/k_f with temperature when temperature is lower than 30°C and a level-off dependence when temperature is higher than 30°C. Duangthongsuk et al. [29] observed a decrease of thermal conductivity ratio from 15°C to 25°C and 35°C in TiO_2 (average diameter of 21 nm) water nanofluids with particle volume fractions from 0.2% to 2% although the nanofluid conductivity k_e increases with temperature. Wang et al. [10] and Wei et al. [12] did not observe a monotonous relationship between k_e/k_f and temperature in their experiments on $CePO_4$-water nanofluids and Cu_2O-water nanofluids, respectively. Therefore, how the nanofluid thermal conductivity depends on its temperature is still an open question.

The particle size dependence of thermal conductivity enhancement is another critical issue that has attracted much attention. The experiment by Chon et al. [47] for Al_2O_3-water nanofluids

Table 2 Summary of experimental data on thermal conductivity enhancement in nanofluids: effects of particle volume fraction, temperature, and particle size (MWCNT: multiwalled carbon nanotube; SWCNT: single-walled carbon nanotube; VGCF: vapor grown carbon fibers; EG: ethylene glycol; EO: engine oil; LI: linear increase with; NI: nonlinear increase with; I: increase with; D: decrease with)

Investigator	Particles	Base fluids	Volume fraction dependence	Temperature dependence	Particle size dependence
Beck et al. [52]	Al_2O_3	Water/EG	-	-	NI, 8–282 nm
Chon et al. [49]	Al_2O_3	Water	-	I, 20–70°C	D, 11/47/150 nm
Das et al. [20]	Al_2O_3/CuO	Water	LI, 1–4%	LI, 20–50°C	-
Lee et al. [24]	Al_2O_3	Water	LI, 1–5%	-	-
Lee et al. [36]	Al_2O_3	Water	LI, 0.01–0.3%	-	-
Li et al. [45]	Al_2O_3	Water	NI, 0.5–6%	LI, 27–37°C	-
Li et al. [52]	Al_2O_3/CuO	Water	LI, 2–10%	LI, 27–36°C	-
Minsta et al. [53]	Al_2O_3/CuO	Water	LI, 1–18%	LI, 22–40°C	-
Zhang et al. [38]	Al_2O_3	Water	NI, 0–15%	No trend (little change), 5–50°C	-
Wei et al. [12]	Cu_2O	Water	No trend	No trend, 10–40°C	-
Philip et al. [54]	Fe_3O_4	Kerosene	Unchange, 0–1.7%; LI, 1.7–8%	-	-
Shima et al. [49]	Fe_3O_4	Water	-	-	LI, 2.8–9.5 nm
Duangthongsuk et al. [29]	TiO_2	Water	LI, 0.2–2%	D, 15/25/35°C	-
Murshed et al. [28]	TiO_2	Water	NI, 0.5–5%	-	-
Murshed et al. [32]	TiO_2/Al_2O_3	Water/EG	LI, 1–5%	I, 20–60°C	-
Xie et al. [34]	SiC	Water/EG	LI, 1–4%	-	-
Murshed et al. [32]	Al	EG/EO	LI, 1–5%	LI, 20–60°C	-
Eastman et al. [26]	Cu	EG	LI, 0–5%	-	-
Patel et al. [18]	Au	Thiolate/citrate	I, 0.00013–0.011%	I, 25–60°C	-
Zhang et al. [38]	Au	Toluene	-	No trend (little change), 5–40°C	-
Patel et al. [18]	Ag	Citrate	-	I, 30–60°C	-
Chopkar et al. [48]	$Al_{70}Cu_{30}$	EG	NI, 0.2–2.5%	-	D, 10–80 nm
Chopkar et al. [21]	Al_2Cu/Ag_2Al	EG	-	-	D, 30–120 nm
Chopkar et al. [21]	Al_2Cu/Ag_2Al	Water	NI, 0.2–1.8%	-	-
Hong et al. [37]	Fe	EG	NI, 0–0.55%	-	D, 1.2–2.3 μm (cluster)
Choi et al. [27]	MWCNT	Oil	NI, 0–1%	-	-
Ding et al. [41]	MWCNT	Water	NI, 0–1 wt%	I, 20/25/30°C	-
Wen et al. [46]	MWCNT	Water	NI	NI	-
Biercuk et al. [42]	SWCNT	Epoxy	No trend, 0–1 wt%	I, 30–280 K; D, 280–300 K	-
Biercuk et al. [42]	VGCF	Epoxy	I, 0–2%	I, 30–180 K D, 180–300 K	-
Wang et al. [10]	$CePO_4$	Water	No trend	No trend, 10–50°C	-

showed that the thermal conductivity ratio k_e/k_f increases when the particle size decreases from 150 nm to 47 nm and 11 nm at a particle volume fraction of 1%. The Brownian motion of nanoparticles was proposed to be the reason behind because smaller particles tend to move more intensively and could thus benefit the thermal transport. A similar trend was observed in Ref. [48] for $Al_{70}Cu_{30}$-EG nanofluids when the particle size varies from 10 nm to 80 nm at a volume fraction of 0.5%. However, the thermal conductivity ratio k_e/k_f was reported to increase as the particle size increases both for magnetite (Fe_3O_4) nanofluids with particles smaller than 10 nm [49] and for Al_2O_3 nanofluids with particle size below 50 nm [50]. This tends to disqualify the effect of particle Brownian motion on thermal conductivity enhancement. It was proposed in Ref. [50] that due to the increase of phonon mean free path in the small sized particles, the nanoparticle thermal conductivity decreases with particle size decrease [51].

Table 2 summarizes the experimental results regarding the effects of particle volume fraction, temperature, and particle size. Clearly, there are wide discrepancies and inconsistencies regarding these parameter effects on thermal conductivity enhancement in nanofluids.

As the pH value decreases, the thermal conductivity ratio k_e/k_f for Al_2O_3-water nanofluids increases [55]. This may come from the enhanced mobility of nanoparticles due to larger difference of the nanofluid pH value from the isoelectric point of Al_2O_3 particle (pH_{iep}=9.2) [55]. A strong sensitivity of conductivity enhancement to the specific surface area of Al_2O_3 nanoparticles was also reported in Ref. [55]. Moreover, Patel et al. [18] detected a less conductivity enhancement for the nanofluid with Au particles coated with a covalent molecular chain (Au-thiolate) than that with uncoated Au particles (Au-citrate). Assael et al. [30] reported that the thermal conductivity enhancement of MWCNT nanofluids also depends on how the MWCNTs are dispersed into the base fluids. Therefore, particle-fluid surface chemical properties also play some role in determining nanofluids thermal conductivity.

3 Mechanisms of Heat Conduction in Nanofluids

The fact that the conventional theory cannot predict the substantially higher thermal conductivity of nanofluids observed in many experiments has inspired efforts in identifying possible mechanisms based on a variety of experimental observations and some numerical simulations. The proposed mechanisms typically fall into two categories: static and dynamic mechanisms. Two popular static or structural mechanisms are the liquid-layering at the particle-liquid interface as heat transfer bridge (Fig. 3(*a*)) and the particle aggregation to form chainlike thermal transport path (Fig. 3(*b*)). The dynamic mechanisms include the particle Brownian motion (Fig. 3(*c*)) and the convection in base fluid induced by the particle Brownian motion (Fig. 3(*d*)).

3.1 Liquid-Layering. The effect of liquid-layering was first proposed in Ref. [27] for explaining the substantially high thermal conductivity in carbon nanotube suspensions. Heat conduction in carbon nanotubes is phonon based [56,57]. The special one-dimensional structure and strong covalent bonds of carbon nanotubes result in a long phonon mean free path and thus a ballistic heat conduction with extremely high thermal conductivity [57–59]. Because of different nature of heat conduction in nano-

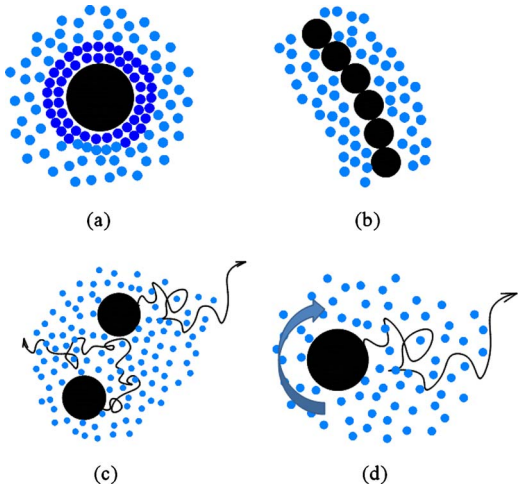

Fig. 3 Sketch of four potential mechanisms responsible for the reported conductivity enhancement: (*a*) liquid-layering, (*b*) particle aggregation, (*c*) particle Brownian motion, and (*d*) Brownian-motion-induced convection

tubes and the base fluid, interfacial thermal resistance may exist at the nanotube-liquid interface [27,60,61]. Near the solid-liquid interface, liquid molecules are more orderly organized [62,63]. It was thus speculated that such organized liquid layers may act as a bridge to generate more effective thermal transport across the interface [27]. Another possibility was proposed in Ref. [64] that if the separation of two particles is so small such that only the organized liquid layer is in between, such solidlike liquid layer may facilitate the ballistic phonons initiated in one particle to persist in the liquid and reach the nearby particle, consequently increasing thermal conductivity. Moreover, the liquid layer itself was speculated to have the better thermal transport ability than the bulk liquid because of its ordered molecular structure [64].

Molecular dynamics (MD) simulations revealed the important role of the liquid-solid interaction strength (described by the Lennard-Jones potential [65]) in determining the interfacial thermal resistance [66,67]. Strong interaction (wetting liquid) results in a strong liquid-layering over several atomic distance and smaller interfacial thermal resistance (inferred from small temperature drop across the interface). Weak interaction (nonwetting liquid) gives a weak liquid-layering over a single layer of liquid atoms and larger thermal resistance (indicated by large temperature drop across the interface) [66,67]. However, the slopes of the temperature profile in liquid were numerically shown to be the same for either highly ordered liquid layer or disordered liquid molecular structure (Fig. 4), thus challenging the hypothesis of the better thermal transport ability in the organized liquid layer than in the bulk liquid [67]. The small thickness of the organized liquid

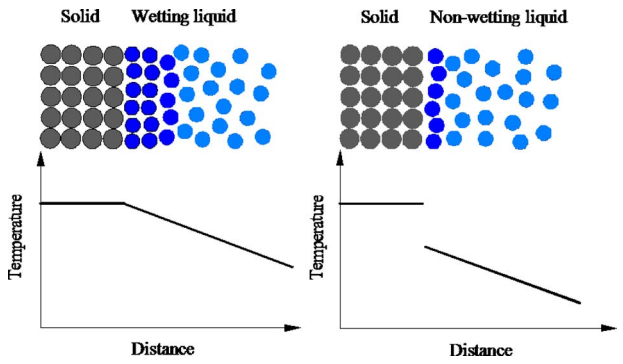

Fig. 4 Temperature profiles for wetting and nonwetting liquids

layer, confirmed both experimentally [62,63] and numerically [67,68], was considered as a possible explanation for its unimproved thermal transport ability [67].

Instead of studying the interface between thin solid slab and liquid film [66,67], another MD simulation was conducted for the particle-liquid interface around small particle aggregates consisting of ten nanoparticles [69]. A percolating network of amorphous-like liquid structure around the aggregates was observed at the presence of a relatively strong particle-liquid interaction (characterized by the well depth ε_{SF} of Lennard-Jones potential [65] relative to the distance ε between the two liquid atoms) [69]. This liquid network was believed to offer a negative interfacial thermal resistance and thus a better thermal transport across the interface than in the bulk liquid [69]. A thermal conductivity increase of 55% was obtained at $\varepsilon_{SF}/\varepsilon=7$ and particle volume fraction $\varphi=3.5\%$ [69]. The inconsistent results between Refs. [67,69] imply the necessity of further study on the effect of interface morphology on liquid layering. Since the simulations in Refs. [67,69] were only for the mono-atomic/molecular base fluids, more research efforts are desirable to examine the liquid-layering effect for the other more complicated base fluids such as water and liquids with molecular chains.

3.2 Particle Aggregation. Particles in nanofluids may aggregate with each other to form chain structures. This has been confirmed experimentally [28,70–73]. Because chain structures allow more heat to transport along the direction of heat flux, the heat conduction could be enhanced due to the particle aggregation [37]. Reviewing these chain-structured aggregates (clusters) as special particles with large aspect ratio, the traditional effective medium theory predicts a higher thermal conductivity of the whole system [74–77]. The network structure induced by the high aspect ratio of nanotubes was also considered as a main reason for the reported extremely high thermal conductivity of the nanotube suspensions [41,78–83]. Recently, Philip et al. [54] and Shima et al. [49] conducted experiments on Fe_3O_4 nanofluids and manipulated particle aggregation structures with variable strength of external magnetic fields. A stronger external magnetic field yields longer particle chain structures in the nanofluids. By increasing the aspect ratio of the linear chains (parallel to the temperature gradient), very large thermal conductivity enhancement were obtained (up to 300% at $\varphi=0.82\%$) [54]. These observations provide the evidence that the aggregate morphology and distribution play an important role in determining thermal conductivity of nanofluids.

3.3 Particle Motion. Particles in nanofluids experience irregular movement, named as Brownian motion, due to the random collisions of the surrounding liquid molecules. The Brownian-motion-induced particle collisions are expected to increase the heat transport among particles (diffusion mode) and thus increase thermal conductivity of the nanofluids [64]. However, the thermal diffusivity of the base fluid is usually two or more orders larger than the particle diffusivity [84]. Therefore, such a Brownian diffusive motion of nanoparticles has a negligible effect on the nanofluid thermal conductivity enhancement [64,85–87].

Another argument is that the Brownian motion of particles may result in convection of the surrounding base fluid and thus enhance the thermal conductivity [85]. Since the Nusselt number around a sphere embedded in a semi-infinite medium equals to 1, the enhanced nanofluid thermal conductivity due to the Brownian motion of a single spherical particle was estimated as $k_e=hr_p$, where h is the convective heat transfer coefficient from an isothermal sphere in the Stokes regime [85]. The calculated thermal conductivity enhancement could reach several percents for a 10 nm Al_2O_3 particle suspended in water or ethylene glycol [85]. This estimation is based on the assumption that the convective velocity of the base fluid is the same as the Brownian velocity of the particle [84]. Intuitively, however, it seems unreasonable to expect such a liquid convective velocity (referring to the liquid bulk mo-

tion on the scale of at least a few molecules) since the particle Brownian motion is just induced by the collisions from neighboring liquid molecules. It was proposed in Ref. [86] that the liquid convective velocity should be on the order of the thermophoretic velocity [88], which offers a negligible effect of liquid convection. The estimation of thermal conductivity enhancement in Ref. [22] also showed an insignificant contribution of either translational- or rotational-Brownian-motion-induced convection [89,90] due to the small Peclet number. There are controversies in existing experiments and simulations; some support the role of particle Brownian motion [20,53,55,48,49] and others disqualify its effect [49,64,87,91].

The motion of nanoparticles is influenced by the collective effect of both Brownian force and other interparticle forces such as van der Waals force and electrostatic force [22]. Kuwabara's cell model [92] was used in Ref. [93] to estimate the contribution of the electrostatic force due to the electrical double layer (EDL) to the nanofluid thermal conductivity, showing a more significant contribution than that from the Brownian-motion-induced particle collisions. Note that the interparticle forces depend on chemical and physical properties of the nanoparticles and the base fluid, as well as the particle morphology and distribution [22]. Also, the interaction among convective currents induced by multiple particles is very complicated [85]. Therefore, it would be very difficult to accurately estimate the effect of particle motion on the thermal conductivity.

3.4 Other Mechanisms. Near-field radiation such as Coulomb interaction was shown to offer an increased thermal conductance between two close particles based on a fluctuating dipole model [94]. With the distance between two particles decreasing to less than the particle diameter, the multipolar contributions can lead to a stronger heat transfer enhancement, which is found to be two to three orders of magnitude more efficient than the enhancement for two contacting particles [94]. However, it was argued in Ref. [95] that the surface electrons in polar nanoparticles play a minor role in the heat-conduction enhancement because the separation distance between particles is comparable with or smaller than the electron wavelength even in nanofluids with a low concentration of particles. The Fourier-diffusion-based experimental data of thermal conductivity were transferred to those corresponding to the hyperbolic heat conduction in Ref. [96], showing that thermal waves in hyperbolic heat conduction could be the source of the excessively improved thermal conductivity of nanofluids. The MD simulation in Ref. [97] showed that a strong short-range nanoparticle-liquid attraction can lead to thermal conductivity enhancement through the excess fluctuation of potential energy.

The fact that the enhancement in thermal properties comes from the presence of nanoparticles has directed research efforts nearly exclusively toward thermal transport at the nanoscale. However, thermal conductivity is actually a macroscale phenomenological characterization of heat conduction. By scaling up the microscale heat-conduction model in the nanoparticles and the base fluid, a dual-phase-lagging heat-conduction model was found to be the governing equation of macroscale heat conduction in nanofluids [10,16,98,99]. Therefore, the molecular physics and the microscale physics in nanofluids manifest themselves as heat diffusion and thermal waves at the macroscale, respectively. The heat diffusion and the thermal waves could either enhance or counteract each other and thus enhance or weaken heat conduction [10,16,98,99].

Addition of 4% of Al_2O_3 particles was reported to increase thermal conductivity by a factor of 8% [24], while CuO particles at the same volume fraction enhance the conductivity by about 12% [6]. This is interesting because conductivity of CuO is less than that of Al_2O_3. The thermal-wave theory can explain this since the conductivity enhancement is strongly affected by nanofluids microstructures and interfacial properties/processes of nanoparticle-fluid interfaces [10,16,99].

Table 3 lists the conductivity ratio k_e/k_f from experiments. It shows that (i) the interaction between the heat diffusion and the thermal waves can either upgrade or downgrade fluid conductivity by the presence of higher-conductivity nanoparticles and (ii) extraordinary water conductivity enhancement (up to 153%) can be achievable by the presence of lower-conductivity oil droplets due to strong thermal waves. The reported strong thermal conductivity enhancement beyond that from the higher value of suspended nanoparticles in Refs. [26,31,48,101–103] is also the evidence of such thermal waves.

Table 3 Measured conductivity ratio k_e/k_f of some nanofluids

Nanofluids	k_e/k_f
$CePO_4$ nanofibers in water [10,16]	0.67–1.54
Cu_2O spherical particles in water [12]	0.83–1.24
Cu_2O octahedral particles in water [12]	0.89–1.24
CuS/Cu_2S hollow spherical particles in water [16]	0.85–1.18
CuS/Cu_2S core-shell spherical particles in water [16]	0.82–1.21
1 vol % alumina nanorods (80×10 nm^2) in water [100]	0.95–1.12
0.001 vol % gold nanoparticles (20–30 nm) in water [100]	0.96–1.08
0.86 vol % Mn–Zn ferrite (12.9 nm) in water [100]	0.95–1.10
Corn oil droplets in water [11]	0.755–2.39
Olive oil droplets in water [10]	0.636–2.533

4 Models for Thermal Conductivity in Nanofluids

4.1 Conventional Models. The prediction of transport properties for heterogeneous mixtures has been back to Maxwell [1]. Thermal conductivity, as one of the transport properties, can be predicted by some conventional static models based on the effective medium theory. This section is on a brief discussion of such models.

Maxwell [1] considered a heterogeneous mixture with very dilute suspension of spherical particles in which the interactions among particles can be ignored. Consider a spherical region of the mixture with spherical particles suspended in the base fluid. The thermal conductivity of the mixture and the base fluid are k_e and k_f, respectively. The whole spherical region is embedded in the same base fluid of thermal conductivity k_f. The temperature T outside the region can be calculated by viewing the spherical region either as a homogenous sphere of conductivity k_e or as a region containing nanoparticles and the base fluid. The effective thermal conductivity ratio k_e/k_f can be thus readily obtained by equalizing the temperature T from the two views:

$$k_e/k_f = 1 + \frac{3\varphi(k_p/k_f - 1)}{k_p/k_f + 2 - \varphi(k_p/k_f - 1)} \tag{1}$$

This equation, known as the Maxwell's equation or Maxwell–Garnett formula, is the basis of many models developed later. Since Maxwell's equation is only a first-order approximation, it works only for mixtures with low particle volume fraction φ and small values of k_p/k_f (less than 10).

Wiener [104] developed both *series mixture rule* and *parallel mixture rule* (Fig. 5):

$$k_e/k_f = 1 + \varphi\frac{k_p/k_f - 1}{k_p/k_f - \varphi(k_p/k_f - 1)} \tag{2}$$

$$k_e/k_f = 1 + \varphi(k_p/k_f - 1) \tag{3}$$

They provide a lower bound and an upper bound for the effective thermal conductivity ratio of a two-phase mixture, respectively. They are also the two special cases of the following general mixture rule at $n=-1$ and $n=1$, respectively [105]:

$$k_e^n = (1-\varphi)k_f^n + \varphi k_p^n \tag{4}$$

Ellipsoidal particles are very important in analyzing the effect of particle geometries on the effective thermal conductivity of mixtures because it is the only case that an approximate expression of the effective thermal conductivity can be obtained analytically [5]. By changing its depolarization factor, ellipsoids can be used to represent other geometries such as spherical, rod-shaped, and needle-shaped particles. Fricke [74] derived the effective thermal conductivity ratio of the ellipsoid suspensions as follows:

$$k_e/k_f = \frac{1-\varphi+\frac{1}{3}\varphi\left(\frac{k_p/k_f}{1+d_{pa}(k_p/k_f+1)}+\frac{k_p/k_f}{1+d_{pb}(k_p/k_f+1)}+\frac{k_p/k_f}{1+d_{pc}(k_p/k_f+1)}\right)}{1-\varphi+\frac{1}{3}\varphi\left(\frac{1}{1+d_{pa}(k_p/k_f+1)}+\frac{1}{1+d_{pb}(k_p/k_f+1)}+\frac{1}{1+d_{pc}(k_p/k_f+1)}\right)} \tag{5}$$

The depolarization factors d_{pa}, d_{pb}, and d_{pc} are defined by

$$d_{pj} = \frac{abc}{2}\int_0^\infty \frac{1}{(j^2+w)\sqrt{(a^2+w)(b^2+w)(c^2+w)}}dw \quad (j=a,b,c) \tag{6}$$

where a, b, and c are the three semi-axes of an ellipsoid.

Bottcher [106] extended Maxwell's equation to high volume fraction case by considering a sphere of mixture embedded in a matrix with a thermal conductivity of k_e, rather than k_f, and thus obtained the following relation:

$$(1-\varphi)\frac{k_f-k_e}{2k_e+k_f}+\varphi\frac{k_p-k_e}{2k_e+k_p}=0 \tag{7}$$

It is usually known as Bruggeman's model because it was first obtained by Bruggeman [107].

Hamilton and Crosser [25] modified Maxwell's equation by introducing an empirical shape factor f_s and thus obtained the following model for k_e/k_f:

$$k_e/k_f = \frac{k_p/k_f+(f_s-1)[1+\varphi(k_p/k_f-1)]}{k_p/k_f+(f_s-1)-\varphi(k_p/k_f-1)} \tag{8}$$

They also fitted the value of f_s from the experimental data and obtained $f_s=3$ for the spherical particle suspensions and $f_s=6$ for the cylindrical particle suspensions. Maxwell's equation is recovered as the special case of the Hamilton–Crosser model for spherical particle suspensions with $f_s=3$.

Hashin and Shtrikman [108] derived the most restrictive lower bound and upper bound of the effective thermal conductivity for macroscopically homogeneous and isotropic multiphase materials by using a variational approach. For two-phase mixture, Hashin and Shtrikman used a composite sphere of radius r_0 consisting of an inner sphere of radius r_1 and thermal conductivity k_p and an outer shell of thermal conductivity k_f to replace a sphere of radius r_0 in an original homogeneous material with thermal conductivity k_e but keep the temperature field outside of r_0-sphere unchanged. k_e can be expressed as a function of k_p, k_f, r_0, and r_1 by solving the Laplace equation with proper boundary conditions. Such changes do not vary the effective thermal conductivity of the original material and can be made indefinitely until all the original material is replaced by composite spheres of infinitesimal size and all with the same value of r_1/r_0. The volume fraction of the k_p material is thus $\varphi=(r_1/r_0)^3$. By applying an inequality deduced from the variational approach, the Hashin-Shtrikman (H-S) upper bound of the effective thermal conductivity for two-phase homogeneous and isotropic mixtures was obtained as

$$k_e/k_f = k_p/k_f\left[1-\frac{3(1-\varphi)(k_p/k_f-1)}{3k_p/k_f-\varphi(k_p/k_f-1)}\right] \tag{9}$$

The H-S lower bound is the same as Maxwell's equation given by Eq. (1). The lower and upper bounds given by Wiener, Eqs. (2) and (3), are actually the least-restrictive bounds for two-phase homogeneous mixtures.

Figure 6 compares the experimental data with the H-S bounds. For oxide nanofluids, some of the data are much lower than the lower bound or much higher than the upper bound. Although the thermal conductivity of CuO (20 W/m °C [109]) is lower than that of Al_2O_3 (40 W/m °C [5]), the thermal conductivity of CuO-water nanofluids is generally higher than that of the Al_2O_3-water nanofluids. For Cu nanofluids and CNT nanofluids, most experimental data fall into the prediction of H-S bounds although the data scatter widely.

A similar analysis can be made for two-dimensional (2D) case to obtain the 2D H-S lower and upper bounds:

$$k_e/k_f|_{\text{lower}} = 1+\frac{2\varphi(k_p/k_f-1)}{k_p/k_f+1-\varphi(k_p/k_f-1)} \tag{10}$$

$$k_e/k_f|_{\text{upper}} = k_p/k_f\left[1-\frac{2(1-\varphi)(k_p/k_f-1)}{2k_p/k_f-\varphi(k_p/k_f-1)}\right] \tag{11}$$

Figure 5 plots the effective thermal conductivity ratio given by the Wiener bounds, H-S bounds, and 2D H-S bounds over the full range of particle volume fraction φ at $k_p/k_f=0.02$ and $k_p/k_f=10$, respectively. The difference between Wiener and H-S bounds becomes smaller when the departure of k_p from k_f gets bigger. The H-S upper bounds (Eqs. (9) and (11)) always correspond to the case that the k_p-phase is continuous and k_f-phase is dispersed (Fig. 5). By contrast, the H-S lower bounds correspond to the case that

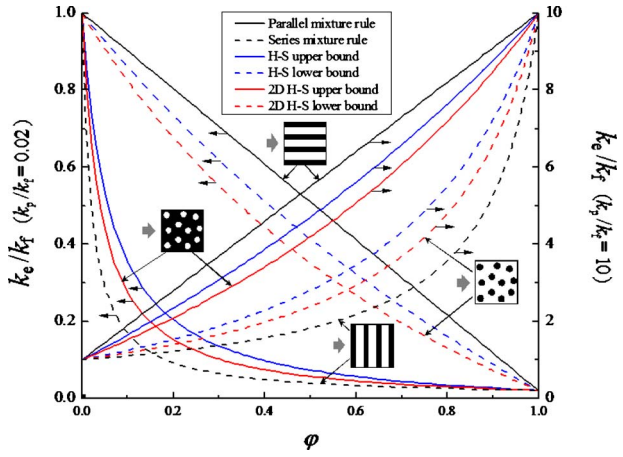

Fig. 5 Comparison among Wiener bounds, H-S bounds, and 2D H-S bounds

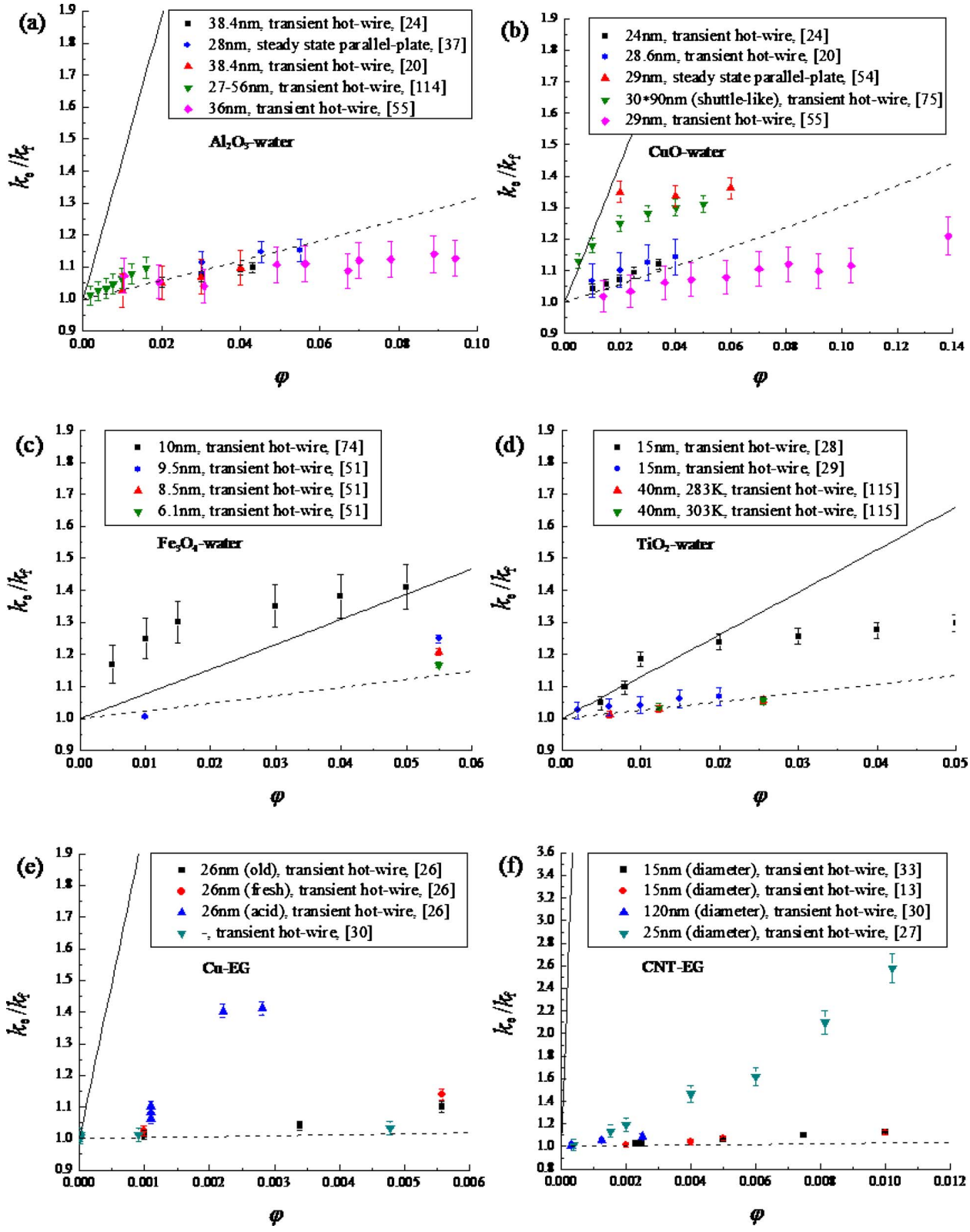

Fig. 6 Comparison between experimental data and H-S bounds (solid line: H-S upper bound; dash line: H-S lower bound) [110,111]

the k_f-phase is continuous and k_p-phase is dispersed. Therefore, we can alter the material conductivity more effectively by organizing the added material in such a way that it forms a continuous phase and disperses the original material as far as possible.

4.2 Recent Models. Since the conventional models are inaccurate to predict the effective thermal conductivity of nanofluids, some new models have been developed by considering one or more potential mechanisms discussed in Sec. 3. As one of the

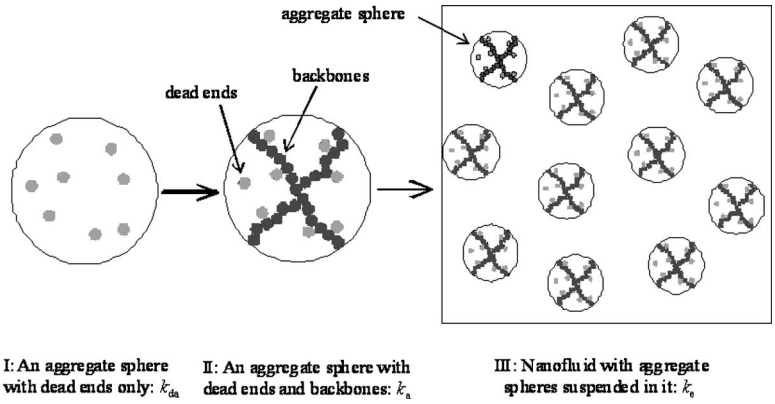

Fig. 7 Schematic of the three-level homogenization theory by Prasher et al. [77]

earliest attempts, Maxwell's model was renovated to include the effect of the organized liquid layer at the particle-liquid interface in Ref. [112] where the thermal conductivity of the layer was set to be 10 or 100 times of that of the bulk liquid or the same as that of the particle, and the layer thickness was set to be 1 or 2 nm. The renovated model successfully predicts some experimental data of CuO and Cu-based nanofluids [112]. The liquid-layering effect has been included by a similar approach in Refs. [32,113–117]. As a modification, a linear distribution of thermal conductivity was imposed in the liquid layer bridging the thermal conductivity of the particle to that of the base fluid in Refs. [118,119]. However, the evaluation of the thickness and thermal conductivity of the liquid layers in these models is still an open question.

The effect of Brownian motion can be included by considering the effective thermal conductivity as a combination of those from the pure conduction and from the Brownian motion [120]. The developed model agreed well with the measured thermal conductivity of Cu-water nanofluids in Ref. [121]. However, the particle aggregation effect was considered to be negligible for the former but significant for the latter in Ref. [120].

Jang et al. [122,123] proposed four modes of energy transport in nanofluids: thermal diffusion in the base fluid, thermal diffusion in nanoparticles, collision between nanoparticles due to the Brownian motion, and thermal interaction between nanoparticles and base fluid molecules, in which the last represents the effect of convection induced by the particle Brownian motion. Since the third mode has been shown to be negligible in Refs. [37,64,85], the effective thermal conductivity k_e was proposed to be calculated by [123]

$$k_e = k_f(1-\varphi) + k_{np}\varphi + C_1 \frac{d_m}{d_p} k_f \ \mathrm{Re}^2 \ \mathrm{Pr}_f \tag{12}$$

Here k_{np} is the thermal conductivity of nanoparticles, which was estimated as 0.01 times that of the bulk solid phase by using the correlation for a single particle in a ballistic heat-conduction model [124] and including the interfacial thermal resistance effect [125]. d_p and d_m are the diameters of the nanoparticle and base fluid molecule, respectively. Re is the Reynolds number based on the nanoparticle Brownian velocity, diameter, and kinetic viscosity of the base fluid. With adjusting the value of empirical constant C_1, their model works well for metallic, oxide, and nanotube nanofluids. A semi-empirical model was proposed in Refs. [85,126], which also includes the effect of Brownian-motion-induced convection:

$$k_e/k_f = (1 + A \ \mathrm{Re}^m \ \mathrm{Pr}_f^{0.333} \ \varphi) \times \left(\frac{[k_p(1+2 \ \mathrm{Bi}) + 2k_f] + 2\varphi[k_p(1-\mathrm{Bi}) - k_f]}{[k_p(1+2 \ \mathrm{Bi}) + 2k_f] - \varphi[k_p(1-\mathrm{Bi}) - k_f]} \right) \tag{13}$$

in which Maxwell's equation was used to estimate the thermal conductivity from pure diffusion but with the interfacial thermal resistance. Here Bi is the nanoparticle Boit number defined as $2R_b k_f / d_p$, where R_b is the experimentally determined interfacial thermal resistance. Furthermore, an empirical formula was also proposed to estimate the effect of Brownian-induced convection [89,118]. Other models considering the effect of Brownian-induced convection include those in Refs. [93,114,127–129]. In these models, there is at least one empirical parameter. As mentioned in Ref. [85], the semi-empirical model seems to be always necessary due to the complexities involved with the interaction in the convective currents among multiple particles.

By using the model in Ref. [76] for predicting effective thermal conductivity of arbitrary particulate composites with interfacial thermal resistance included, Nan et al. [130] developed a simple formula to show that the ultrahigh thermal conductivity and large aspect ratio of nanotubes contribute to the significant increase of the effective thermal conductivity, while the interface thermal resistance at the nanotube-liquid interface causes a degradation in the thermal conductivity enhancement. Other models for prediction of effective thermal conductivity of nanotube suspensions include those in Refs. [78,81–83]. A common result can be drawn from these models that both the nanotube geometry and interfacial thermal resistance play important roles in heat-conduction process. Moreover, all these models were developed based on the conventional effective medium approach and the ellipsoidal geometrical model without involving any new mechanisms.

Prasher et al. [77] developed a three-level homogenization theory to study the effect of particle aggregation on the conductivity enhancement in nanofluids. They used the fractal theory to correlate the aggregates' morphology and distribution to the chemical and fractal dimensions of the aggregates [115]. In Ref. [77], some suspended particles are assumed to form linear chains (backbones, Fig. 7) spanning the whole aggregate spheres; the others form the side chains (dead ends, Fig. 7). At the first level of homogenization, Bruggeman's model was used to calculate the effective thermal conductivity of the aggregate with the presence of the dead-end particles only,

$$(1-\varphi_{da})\frac{k_f-k_{da}}{2k_{da}+k_f}+\varphi_{da}\frac{k_p-k_{da}}{2k_{da}+k_p}=0 \tag{14}$$

Here k_{da} is the thermal conductivity of the dead-end particles. φ_{da} is the volume fraction of the dead-end particles in the aggregate spheres, given by $(R_g/r_p)^{d_f-3}-(R_g/r_p)^{d_l-3}$ with R_g, r_p, d_l, and d_f as the aggregate radius of gyration, radius of nanoparticles, and chemical and fractal dimensions of the aggregate, respectively. At the second level, the model for randomly oriented cylindrical particles [76] (Eq. (14)) was used to estimate the effective thermal conductivity of the whole aggregate sphere with both backbones and dead ends,

$$k_a=k_{da}\frac{3+\varphi_{ca}[2\beta_{11}(1-L_{11})+\beta_{33}(1-L_{33})]}{3-\varphi_{ca}(2\beta_{11}L_{11}+\beta_{33}L_{33})} \tag{15}$$

where φ_{ca} is the volume fraction of the linear chains in the aggregate sphere, given by $(R_g/r_p)^{d_l-3}$. L_{11} and L_{33} are the two particle-shape dependent parameters. β_{11} and β_{33} are the effective thermal conductivities along two principle axes of the ellipsoid, respectively, which are functions of the geometrical parameters and thermal conductivities of the particles and base fluid. Finally, the effective thermal conductivity of nanofluids was calculated by using Maxwell's equation:

$$k_e/k_f=1+3\varphi_a\frac{k_a/k_f-1}{k_a/k_f+2-\varphi_a(k_a/k_f-1)} \tag{16}$$

in which φ_a and k_a are the volume fraction and effective thermal conductivity of aggregates, respectively. For the known particle volume fraction φ, particle geometry, particle and base fluid conductivities, and either R_g or φ_a, the model can predict the effective thermal conductivity of nanofluids. The results show that the effective thermal conductivity can be significantly enhanced by the particle aggregation. This model was further extended by using the colloidal chemistry to refine the aggregation kinetics and including the effect of both Brownian-motion-induced convection and interfacial thermal resistance [131,132]. Such an extension shows that the thermal conductivity depends not only on particle size and temperature but also on chemical parameters such as Hamaker constant, zeta-potential, pH value, and ion concentration. The thermal conductivity can also be degraded by the interfacial thermal resistance. The model appears very promising. However, it involves several empirical parameters and more experimental data are needed to verify its accuracy.

For transport in nanofluids, several different length scales are involved: molecular scale, microscale, macroscale, and system scale. The classical heat-conduction equation has usually been postulated as the macroscale model but without adequate justification. A macroscale heat-conduction model in nanofluids has been developed in Refs. [10,16,133] by scaling up the microscale model for heat conduction in nanoparticles and in base fluids, which consists of Fourier law of heat conduction and energy conservation equation. The approach for scaling up is the volume averaging [134–136] with the help of multiscale theorems [136]. Without considering the effects of interfacial thermal resistance and dynamic processes on particle-fluid interfaces, the macroscale heat-conduction equation reads

$$\frac{\partial\langle T_i\rangle^i}{\partial t}+\tau_q\frac{\partial^2\langle T_i\rangle^i}{\partial t^2}=\alpha\Delta\langle T_i\rangle^i+\alpha\tau_T\frac{\partial}{\partial t}(\Delta\langle T_i\rangle^i)+\frac{\alpha}{k_e}\left[F(\mathbf{r},t)+\tau_q\frac{\partial F(\mathbf{r},t)}{\partial t}\right] \tag{17a}$$

where

$$\tau_q=\frac{\gamma_f\gamma_p}{ha_v(\gamma_f+\gamma_p)} \tag{17b}$$

$$\tau_T=\frac{\gamma_f k_{pp}+\gamma_p k_{ff}}{ha_v(k_{ff}+k_{pp}+2k_{fp})} \tag{17c}$$

$$k_e=k_{ff}+k_{pp}+2k_{fp} \tag{17d}$$

$$\alpha=\frac{k_{ff}+k_{pp}+2k_{fp}}{\gamma_f+\gamma_p} \tag{17e}$$

$$\begin{aligned}F(\mathbf{r},t)+\tau_q\frac{\partial F(\mathbf{r},t)}{\partial t}=\frac{1}{ha_v}\Big\{&(k_{fp}^2-k_{ff}k_{pp})\Delta^2\langle T_i\rangle^i\\&+\left[\gamma_f\frac{\partial}{\partial t}(\mathbf{u}_{pp}\cdot\nabla\langle T_i\rangle^i)+\gamma_p\frac{\partial}{\partial t}(\mathbf{u}_{ff}\cdot\nabla\langle T_i\rangle^i)\right]\\&-\{k_{pp}\Delta(\mathbf{u}_{ff}\cdot\nabla)+k_{ff}\Delta(\mathbf{u}_{pp}\cdot\nabla)-k_{pf}\Delta(\mathbf{u}_{fp}\cdot\nabla)\\&-k_{fp}\Delta(\mathbf{u}_{pf}\cdot\nabla)\}\langle T_i\rangle^i-[(\mathbf{u}_{ff}\cdot\nabla)(\mathbf{u}_{pp}\cdot\nabla)\\&-(\mathbf{u}_{fp}\cdot\nabla)(\mathbf{u}_{pf}\cdot\nabla)]\langle T_i\rangle^i\Big\}\end{aligned} \tag{17f}$$

Here $\langle T_i\rangle^i$ is the intrinsic average temperature in the i-phase (i=f,p; f and p stand for fluid and particle, respectively) [10,16,133,134]. t is the time. τ_q and τ_T are the phase lags of the heat flux and the temperature gradient, respectively [10,98,99,136,137]. $\gamma_f=(1-\varphi)(\rho c)_f$ and $\gamma_p=\varphi(\rho c)_p$ are the effective thermal capacities in the base fluid and particles, respectively, with ρ and c as the density and specific heat, respectively. k_{ff}, k_{pp}, k_{fp}, ha_v, $\mathbf{u}_{ff}$, $\mathbf{u}_{pp}$, $\mathbf{u}_{fp}$, and $\mathbf{u}_{pf}$ are the macroscopic coefficients that represent the effects of microscale physics on macroscale properties [16,138]. Therefore, the presence of nanoparticles shifts the Fourier heat conduction in the base fluid into the dual-phase-lagging heat conduction in nanofluids at the macroscale [10,16,133]. Consider

$$\frac{\tau_T}{\tau_q}=1+\frac{\gamma_f^2k_{pp}+\gamma_p^2k_{ff}-2\gamma_f\gamma_pk_{fp}}{\gamma_f\gamma_pk_e} \tag{18}$$

It can be larger, equal, or smaller than 1 depending on the sign of $\gamma_f^2k_{pp}+\gamma_p^2k_{ff}-2\gamma_f\gamma_pk_{fp}$. By the condition for the existence of thermal waves that requires $\tau_T/\tau_q<1$ [99,139], we may have thermal waves in nanofluid heat conduction when $\gamma_f^2k_{pp}+\gamma_p^2k_{ff}-2\gamma_f\gamma_pk_{fp}<0$. Depending on the detailed microscale physics in nanofluids, the heat diffusion and thermal waves may either enhance or counteract each other and thus enhance or weaken heat conduction. Focused efforts are thus in great demand to find the correlation between the microscale physics and macroscale properties through solving the closure problems for the four macroscopic thermal coefficients k_{ff}, k_{pp}, k_{fp}, and ha_v. The first attempt of such efforts has been recently made in Ref. [140] to examine how particle-fluid conductivity ratio, particle volume fraction, and shape affect the macroscale thermal properties for nanofluids consisting of in-line arrays of perfectly dispersed two-dimensional circular, square, and hollow particles (represented by the unit cells in Figs. 8(*a*)–8(*c*)). In these simple and perfectly dispersed nanofluids, the heat conduction is diffusion dominant so that the effective thermal conductivity can be predicted adequately by the mixture rule (Eq. (4)) with the effect of particle shape and particle-fluid conductivity ratio incorporated into its empirical parameter [140]. Parameter n in the mixture rule from the fitting of numerical results is listed in Table 4 for three nanoparticle suspensions [140].

The effects of particle size distribution, particle aggregation, and aggregate morphology have also been studied in Ref. [141] for seven kinds of nanofluids containing in-line and staggered arrays of circular cylinders, in-line arrays of cross cylinders, square- and cross-aggregations, hollow cylinders, and cross-particle networks, respectively (represented by the unit cells in Figs. 8(*c*)–8(*i*)). The radius of gyration of particles R_g and the nondimensional particle-fluid interfacial area in the unit cell η (all

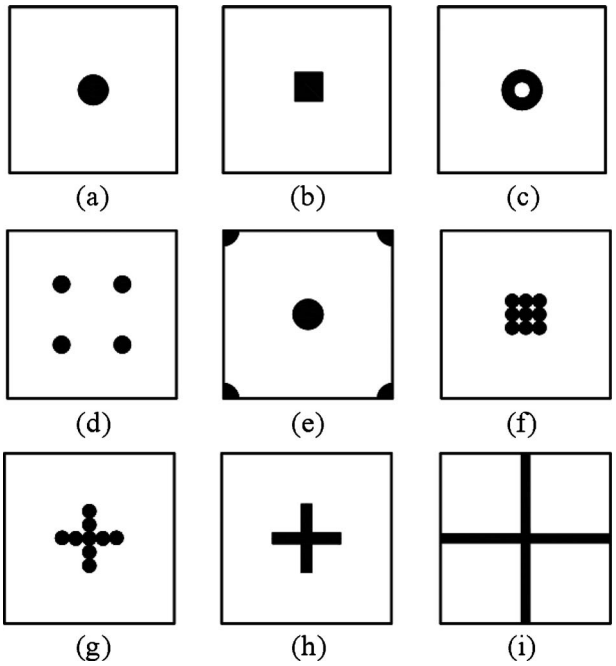

Fig. 8 Unit cells representing nanofluids containing in-line arrays of ((*a*) and (*d*)) circular cylinders, (*b*) square cylinders, (*c*) hollow cylinders, (*e*) staggered arrays of circular cylinders, ((*f*) and (*g*)) in-line arrays of circular particle aggregates, (*h*) cross cylinders, and (*i*) cross-particle networks

dimensions are normalized by the dimension of the unit cell; η thus depends on the geometry of the particle) are found to be two very important parameters in characterizing the effect of particles' geometrical structures on the nanofluid thermal conductivity because for two particles with different shapes (hollow and cross) but the same R_g and η, their macroscopic thermal coefficients are almost the same (Fig. 9, in which l_u is the dimension of the unit cell) [141]. The increase of either R_g or η could result in a larger increase (decrease) of k_e/k_f when $k_p/k_f>1$ (<1) [141]. As a limit case, cross-network particles in Fig. 8(*i*) have a maximal radius of gyration, form a network, and separate the base fluid to become the dispersed phase. Nanofluids with such cross-network particles have a very high (low) thermal conductivity when $k_p/k_f>1$ (<1). Their conductivity can actually reach the 2D H-S upper bound (Fig. 10). Therefore, future efforts should focus on the synthesis of nanofluids containing particles/aggregates with large R_g and η to maximize the effect of added particles on the conductivity enhancement.

The model can be further extended by including the effect of

Table 4 Parameter *n* in the mixture rule from the fitting of numerical results [140]

Particle shape	n
Circular	$-0.46+\dfrac{0.91}{1+\exp\left(\dfrac{\ln(k_p/k_f)}{1.38}+0.063\right)}$
Square	$-0.44+\dfrac{0.86}{1+\exp\left(\dfrac{\ln(k_p/k_f)}{1.45}+0.038\right)}$
Hollow	$-0.42+\dfrac{0.84}{1+\exp\left(\dfrac{\ln(k_p/k_f)}{2.84}-0.058\right)}$

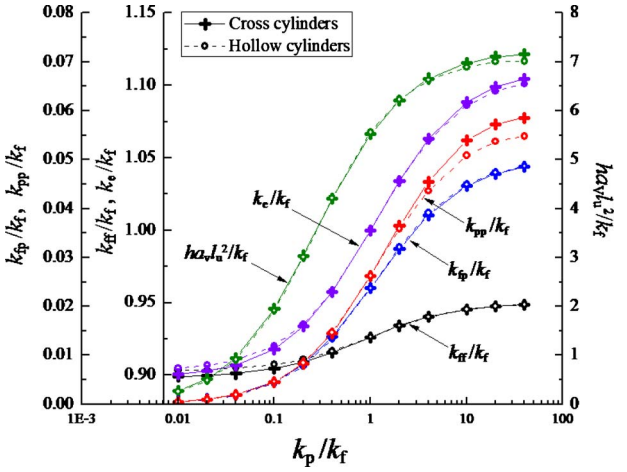

Fig. 9 Macroscale thermal coefficients for the two particles with the same surface-to-volume ratio, radius of gyration, and volume fraction (φ=0.05)

interfacial thermal resistance, dynamic processes on particle-fluid interfaces, and convection [16,142]. Note that this first-principles model was rigorously derived from the microscale model without any adjustable or empirical parameters involved.

5 Concluding Remarks

The present work offers an overview of the recent research and development on heat conduction in nanofluids with an emphasis on their thermal conductivity (experimental data, proposed mechanisms responsible for conductivity enhancement and predicting models). Nanofluids with suspended oxide, metallic particles, and carbon nanotubes have been the focus of experiments. The metallic nanoparticle and nanotube suspensions seem to exhibit more promising conductivity enhancement than the oxide particle suspensions. Many experiments show a higher thermal conductivity of nanofluids than the prediction from the conventional models such as Maxwell's equation and Hamilton–Crosser model. Also observed is the anomalously lower thermal conductivity of nanofluids than that of the base fluids. Therefore, heat conduction in nanofluids is nonconventional. Moreover, the conductivity enhancement depends not only on the particle volume

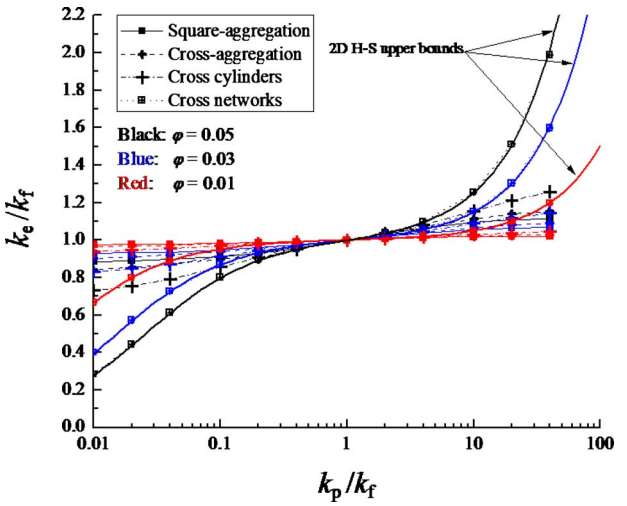

Fig. 10 Effective thermal conductivity of four nanofluids: a comparison between the numerical results and the 2D H-S upper bounds

fraction and particle-fluid conductivity ratio but also on the particle size, temperature, and chemical and interfacial properties on the particle-fluid interface.

The proposed mechanisms for explaining experimental observations include the liquid-layering at the particle-liquid interfaces, the particle aggregation, and the Brownian motion of nanoparticles. The liquid-layering effect is unsupported by several studies, which showed that the thickness of the liquid layer is too small to play a significant role. All successful predictions by considering this effect depend on proper selection of some empirical parameters such as thermal conductivity and thickness of liquid layers. Both experimental data and theoretical analysis show a positive effect of particle aggregation on the enhancement of nanofluid thermal conductivity. Since the particle aggregation depends on many factors, all existing models of predicting its effect contain some empirical parameters. The literature tends to disqualify the effect of particles' collision due to the Brownian motion. The effect of Brownian-motion-induced convection has also been studied. However, whether the particle Brownian motion could induce bulk motion of the surrounding base fluid is still an open question. The particle motion also depends on other interparticle forces such as van der Waals force and electrostatic force, which further complicate the evaluation of particle motion effect.

A recently developed thermal-wave theory predicts a dual-phase-lagging heat conduction in nanofluids at the macroscale. Therefore, the heat-conduction process could be either diffusion dominant or thermal wave dominant depending on microscale physics of nanofluids. The experimental evidence of such thermal waves includes the abnormally lower thermal conductivity of solid particle suspensions and higher thermal conductivity of oil droplet suspensions compared with the base fluids. The thermal-wave theory provides the possibility to rigorously study how the microscale physics affects the macroscale heat conduction in nanofluids. The numerical simulation based on this theory shows that the theory works very well and identifies the particle radius of gyration and nondimensional particle-fluid interfacial area in the unit cell as the two characterizing parameters of governing the effect of particle geometry on effective thermal conductivity of nanofluids.

Acknowledgment

The financial support from the Research Grants Council of Hong Kong (Grant Nos. GRF718009 and GRF717508) is gratefully acknowledged.

References

[1] Maxwell, J. C., 1873, *Treatise on Electricity and Magnetism*, Clarendon, Oxford.
[2] Maxwell, J. C., 1881, *A Treatise on Electricity and Magnetism*, Vol. 1, 2nd ed., Clarendon, Oxford.
[3] Choi, S. U. S., and Eastman, J. A., 1995, "Enhancing Thermal Conductivity of Fluids With Nanoparticles," *Developments and Applications of Non-Newtonian Flows*, D. A. Siginer and H. P. Wang, eds., ASME, New York, **FED-231**, pp. 99–105.
[4] Das, S. K., Choi, S. U. S., and Patel, H. E., 2006, "Heat Transfer in Nanofluids—A Review," Heat Transfer Eng., **27**(10), pp. 3–19.
[5] Das, S. K., Choi, S. U. S., Yu, W., and Pradeep, T., 2008, *Nanofluids: Science and Technology*, Wiley, Hoboken, NJ.
[6] Eastman, J. A., Phillpot, S. R., Choi, S. U. S., and Keblinski, P., 2004, "Thermal Transport in Nanofluids," Annu. Rev. Mater. Res., **34**, pp. 219–246.
[7] Kakaç, S., and Pramuanjaroenkij, A., 2009, "Review of Convective Heat Transfer Enhancement With Nanofluids," Int. J. Heat Mass Transfer, **52**, pp. 3187–3196.
[8] Keblinski, P., Eastman, J. A., and Cahill, D. G., 2005, "Nanofluids for Thermal Transport," Mater. Today, **8**(6), pp. 36–44.
[9] Wang, X. Q., and Mujumdar, A. S., 2007, "Heat Transfer Characteristics of Nanofluids: A Review," Int. J. Therm. Sci., **46**, pp. 1–19.
[10] Wang, L. Q., and Wei, X., 2009, "Nanofluids: Synthesis, Heat Conduction, and Extension," ASME J. Heat Transfer, **131**, pp. 033102.
[11] Wei, X. H., and Wang, L. Q., 2009, "1+1>2: Extraordinary Fluid Conductivity Enhancement," Curr. Nanosci., **5**, pp. 527–529.
[12] Wei, X., Zhu, H., Kong, T., and Wang, L. Q., 2009, "Synthesis and thermal Conductivity of Cu2O Nanofluids," Int. J. Heat Mass Transfer, **52**, pp. 4371–4374.
[13] Liu, M. S., Lin, M. C. C., Huang, I. T., and Wang, C. C., 2005, "Enhancement of Thermal Conductivity With Carbon Nanotube for Nanofluids," Int. Commun. Heat Mass Transfer, **32**(9), pp. 1202–1210.
[14] Choi, S. U. S., Zhang, Z. G., and Keblinski, P., 2004, "Nanofluids," *Encyclopedia of Nanoscience and Nanotechnology*, H. S. Nalwa, ed., American Scientific, Valencia, CA, pp. 757–773.
[15] Peterson, G. P., and Li, C. H., 2006, "Heat and Mass Transfer in Fluids With Nanoparticle Suspensions," Adv. Heat Transfer, **39**, pp. 257–376.
[16] Wang, L. Q., and Quintard, M., 2009, "Nanofluids of the Future," *Advances in Transport Phenomena*, Springer, New York, pp. 179–243.
[17] Davis, W. R., 1984, "Hot-Wire Method for the Measurement of the Thermal Conductivity of Refractory Materials," *Compendium of Thermophysical Property Measurement Method*, Vol. 1, K. Maglic, A. Cezairliyan, and V. Peletsky, eds., Plenum, New York, pp. 231–254.
[18] Patel, H. E., Das, S. K., Sundararajan, T., Sreekumaran, N. A., George, B., and Pradeep, T., 2003, "Thermal Conductivities of Naked and Monolayer Protected Metal Nanoparticle Based Nanofluids: Manifestation of Anomalous Enhancement and Chemical Effects," Appl. Phys. Lett., **83**(14), pp. 2931–2933.
[19] Assael, M. J., Antoniadis, K. D., and Tzetzis, D., 2008, "The Use of the Transient Hot-Wire Technique for Measurement of the Thermal Conductivity of an Epoxy-Resin Reinforced With Glass Fibres and/or Carbon Multi-Walled Nanotubes," Compos. Sci. Technol., **68**, pp. 3178–3183.
[20] Das, S. K., Putra, N., Thiesen, P., and Roetzel, W., 2003, "Temperature Dependence of Thermal Conductivity Enhancement for Nanofluids," ASME J. Heat Transfer, **125**(4), pp. 567–574.
[21] Chopkar, M., Sudarshan, S., Das, P. K., and Manna, I., 2008, "Effect of Particle Size on Thermal Conductivity of Nanofluids," Metall. Mater. Trans. A, **39**, pp. 1535–1542.
[22] Wang, X., Xu, X., and Choi, S. U. S., 1999, "Thermal Conductivity of Nanoparticle-Fluid Mixture," J. Thermophys. Heat Transfer, **13**(4), pp. 474–480.
[23] Masuda, H., Ebata, A., Teramae, K., and Hishinuma, N., 1993, "Alteration of Thermal Conductivity and Viscosity of Liquid by Dispersing Ultra-Fine Particles (Dispersion of Al2O3, SiO2, and TiO2 Ultra-Fine Particles)," Netsu Bussei, **4**(4), pp. 227–233.
[24] Lee, S. P., Choi, S. U. S., Li, S., and Eastman, J. A., 1999, "Measuring Thermal Conductivity of Fluids Containing Oxide Nanoparticles," ASME J. Heat Transfer, **121**, pp. 280–289.
[25] Hamilton, R. L., and Crosser, O. K., 1962, "Thermal Conductivity of Heterogeneous Two-Component Systems," Ind. Eng. Chem. Fundam., **1**(3), pp. 187–191.
[26] Eastman, J. A., Choi, S. U. S., Li, S., Yu, W., and Thompson, L. J., 2001, "Anomalously Increased Effective Thermal Conductivities of Ethylene Glycol-Based Nanofluids Containing Copper Nanoparticles," Appl. Phys. Lett., **78**(6), pp. 718–720.
[27] Choi, S. U. S., Zhang, Z. G., Yu, W., Lockwood, F. E., and Grulke, E. A., 2001, "Anomalous Thermal Conductivity Enhancement in Nanotube Suspensions," Appl. Phys. Lett., **79**(14), pp. 2252–2254.
[28] Murshed, S. M. S., Leong, K. C., and Yang, C., 2005, "Enhanced Thermal Conductivity of TiO2-Water Based Nanofluids," Int. J. Therm. Sci., **44**(4), pp. 367–373.
[29] Duangthongsuk, W., and Wongwises, S., 2009, "Measurement of Temperature-Dependent Thermal Conductivity and Viscosity of TiO2-Water Nanofluids," Exp. Therm. Fluid Sci., **33**, pp. 706–714.
[30] Assael, M. J., Metaxa, I. N., Kakosimos, K., and Constantinou, D., 2006, "Thermal Conductivity of Nanofluids—Experimental and Theoretical," Int. J. Thermophys., **27**(4), pp. 999–1017.
[31] Hong, T. K., Yang, H. S., and Choi, C. J., 2005, "Study of the Enhanced Thermal Conductivity of Fe Nanofluids," J. Appl. Phys., **97**(6), p. 064311.
[32] Murshed, S. M. S., Leong, K. C., and Yang, C., 2008, "Investigations of Thermal Conductivity and Viscosity of Nanofluids," Int. J. Therm. Sci., **47**, pp. 560–568.
[33] Xie, H., Lee, H., Youn, W., and Choi, M., 2003, "Nanofluids Containing Multiwalled Carbon Nanotubes and Their Enhanced Thermal Conductivities," J. Appl. Phys., **94**(8), pp. 4967–4971.
[34] Xie, H., Wang, J., Xi, T., and Liu, Y., 2002, "Thermal Conductivity of Suspensions Containing Nanosized SiC Particles," Int. J. Thermophys., **23**(2), pp. 571–580.
[35] Putnam, S. A., Cahill, D. G., and Braun, P. V., 2006, "Thermal Conductivity of Nanoparticle Suspensions," J. Appl. Phys., **99**, pp. 084308.
[36] Lee, J. H., Hwang, K. S., Jang, S. P., Lee, B. H., Kim, J. H., Choi, S. U. S., and Choi, C. J., 2008, "Effective Viscosities and Thermal Conductivities of Aqueous Nanofluids Containing Low Volume Concentrations of Al2O3 Nanoparticles," Int. J. Heat Mass Transfer, **51**, pp. 2651–2656.
[37] Hong, K. S., Hong, T. K., and Yang, H. S., 2006, "Thermal Conductivity of Fe Nanofluids Depending on the Cluster Size of Nanoparticles," Appl. Phys. Lett., **88**(3), p. 031901.
[38] Zhang, X., Gu, H., and Fujii, M., 2007, "Effective Thermal Conductivity and Thermal Diffusivity of Nanofluids Containing Spherical and Cylindrical Nanoparticles," Exp. Therm. Fluid Sci., **31**(6), pp. 593–599.
[39] Assael, M. J., Chen, C. F., Metaxa, I., and Wakeham, W. A., 2004, "Thermal Conductivity of Suspensions of Carbon Nanotubes in Water," Int. J. Thermophys., **25**(4), pp. 971–985.
[40] Assael, M. J., Metaxa, I. N., Arvanitidis, J., Christofilos, D., and Lioutas, C., 2005, "Thermal Conductivity Enhancement in Aqueous Suspensions of Carbon Multi-Walled and Double-Walled Nanotubes in the Presence of Two Different Dispersants," Int. J. Thermophys., **26**(3), pp. 647–664.

[41] Ding, Y. L., Alias, H., Wen, D. S., and Williams, R. A., 2006, "Heat Transfer of Aqueous Suspensions of Carbon Nanotubes (CNT Nanofluids)," Int. J. Heat Mass Transfer, **49**(1–2), pp. 240–250.
[42] Biercuk, M. J., Llaguno, M. C., Radosavljevic, M., Hyun, J. K., Johnson, A. T., and Fischer, J. E., 2002, "Carbon Nanotube Composites for Thermal Management," Appl. Phys. Lett., **80**(15), pp. 2767–2769.
[43] Chen, H., Yang, W., He, Y., Ding, Y., Zhang, L., Tan, C., Lapkin, A. A., and Bavykin, D. V., 2008, "Heat Transfer and Flow Behaviour of Aqueous Suspensions of Titanate Nanotubes (Nanofluids)," Powder Technol., **183**, pp. 63–72.
[44] Cao, B. Y., and Guo, Z. Y., 2007, "Equation of Motion of a Phonon Gas and Non-Fourier Heat Conduction," J. Appl. Phys., **102**, p. 053503.
[45] Li, C. H., and Peterson, G. P., 2007, "The Effect of Particle Size on the Effective Thermal Conductivity of Al2O3-Water Nanofluids," J. Appl. Phys., **101**, p. 044312.
[46] Wen, D. S., and Ding, Y. L., 2004, "Effective Thermal Conductivity of Aqueous Suspensions of Carbon Nanotubes (Carbon Nanotubes Nanofluids)," J. Thermophys. Heat Transfer, **18**(4), pp. 481–485.
[47] Chon, C. H., Kihm, K. D., Lee, S. P., and Choi, S. U. S., 2005, "Empirical Correlation Finding the Role of Temperature and Particle Size for Nanofluid (Al2O3) Thermal Conductivity Enhancement," Appl. Phys. Lett., **87**, p. 153107.
[48] Chopkar, M., Das, P. K., and Manna, I., 2006, "Synthesis and Characterization of Nanofluid for Advanced Heat Transfer Applications," Scr. Mater., **55**(6), pp. 549–552.
[49] Shima, P. D., Philip, J., and Raj, B., 2009, "Role of Microconvection Induced by Brownian Motion of Nanoparticles in the Enhanced Thermal Conductivity of Stable Nanofluids," Appl. Phys. Lett., **94**, p. 223101.
[50] Beck, M. P., Yuan, Y. H., Warrier, P., and Teja, A. S., 2009, "The Effect of Particle Size on the Thermal Conductivity of Alumina Nanofluids," J. Nanopart. Res., **11**(5), pp. 1129–1136.
[51] Fang, K. C., Weng, C. I., and Ju, S. P., 2006, "An Investigation Into the Structural Features and Thermal Conductivity of Silicon Nanoparticles Using Molecular Dynamics Simulations," Nanotechnology, **17**(15), pp. 3909–3914.
[52] Li, C. H., and Peterson, G. P., 2006, "Experimental Investigation of Temperature and Volume Fraction Variations on the Effective Thermal Conductivity of Nanoparticle Suspensions (Nanofluids)," J. Appl. Phys., **99**(8), p. 084314.
[53] Mintsa, H. A., Roy, G., Nguyen, C. T., and Doucet, D., 2009, "New Temperature Dependent Thermal Conductivity Data for Water-Based Nanofluids," Int. J. Therm. Sci., **48**, pp. 363–371.
[54] Philip, J., Shima, P. D., and Raj, B., 2008, "Evidence for Enhanced Thermal Conduction Through Percolating Structures in Nanofluids," Nanotechnology, **19**, p. 305706.
[55] Xie, H., Wang, J., Xi, T., Liu, Y., and Ai, F., 2002, "Thermal Conductivity Enhancement of Suspensions Containing Nanosized Alumina Particles," J. Appl. Phys., **91**(7), pp. 4568–4572.
[56] Hone, J., 2004, "Carbon Nanotubes: Thermal Properties," J. Nanosci. Nanotechnol., **6**, pp. 603–610.
[57] Shiomi, J., and Maruyama, S., "Diffusive-Ballistic Heat Conduction of Carbon Nanotubes and Nanographene Ribbons," Int. J. Thermophys., in press.
[58] Hone, J., Whitney, M., and Zettl, A., 1999, "Thermal Conductivity of Single-Walled Carbon Nanotubes," Synth. Met., **103**(1–3), pp. 2498–2499.
[59] Berber, S., Kwon, Y. K., and Tomanek, D., 2000, "Unusually High Thermal Conductivity of Carbon Nanotubes," Phys. Rev. Lett., **84**(20), pp. 4613–4616.
[60] Chen, G., 2000, "Particularities of Heat Conduction in Nanostructures," J. Nanopart. Res., **2**, pp. 199–204.
[61] Huxtable, S. T., Cahill, D. G., Shenogin, S., Xue, L. P., Ozisik, R., Barone, P., Usrey, M., Strano, M. S., Siddons, G., Shim, M., and Keblinski, P., 2003, "Interfacial Heat Flow in Carbon Nanotube Suspensions," Nature Mater., **2**(11), pp. 731–734.
[62] Yu, C. J., Richter, A. G., Datta, A., Durbin, M. K., and Dutta, P., 1999, "Observation of Molecular Layering in Thin Liquid Films Using X-Ray Reflectivity," Phys. Rev. Lett., **82**(11), pp. 2326–2329.
[63] Yu, C. J., Richter, A. G., Datta, A., Durbin, M. K., and Dutta, P., 2000, "Molecular Layering in a Liquid on a Solid Substrate: An X-Ray Reflectivity Study," Physica B, **283**(1–3), pp. 27–31.
[64] Keblinski, P., Phillpot, S. R., Choi, S. U. S., and Eastman, J. A., 2002, "Mechanisms of Heat Flow in Suspensions of Nano-Sized Particles (Nanofluids)," Int. J. Heat Mass Transfer, **45**, pp. 855–863.
[65] Lennard-Jones, J. E., and Devonshire, A. F., 1937, "Critical Phenomena in Gases. I," Proc. R. Soc. London, Ser. A, **163**(912), pp. 53–70.
[66] Xue, L., Keblinski, P., Phillpot, S. R., Choi, S. U. S., and Eastman, J. A., 2003, "Two Regimes of Thermal Resistance at a Liquid-Solid Interface," J. Chem. Phys., **118**(1), pp. 337–339.
[67] Xue, L., Keblinski, P., Phillpot, S. R., Choi, S. U. S., and Eastman, J. A., 2004, "Effect of Liquid Layering at the Liquid-Solid Interface on Thermal Transport," Int. J. Heat Mass Transfer, **47**, pp. 4277–4284.
[68] Henderson, J. R., and Vanswol, F., 1984, "On the Interface Between a Fluid and a Planar Wall—Theory and Simulations of a Hard-Sphere Fluid at a Hard-Wall," Mol. Phys., **51**(4), pp. 991–1010.
[69] Eapen, J., Li, J., and Yip, S., 2007, "Beyond Maxwell Limit: Thermal Conduction in Nanofluids With Percolating Fluid Structures," Phys. Rev. E, **76**, p. 062501.
[70] Kim, S. H., Choi, S. R., and Kim, D., 2007, "Thermal Conductivity of Metal-Oxide Nanofluids: Particle Size Dependence and Effect of Laser Irradiation," ASME J. Heat Transfer, **129**(3), pp. 298–307.
[71] Liu, M. S., Lin, M. C. C., Tsai, C. Y., and Wang, C. C., 2006, "Enhancement of Thermal Conductivity With Cu for Nanofluids Using Chemical Reduction Method," Int. J. Heat Mass Transfer, **49**(17–18), pp. 3028–3033.
[72] Zhu, H. T., Zhang, C. Y., Liu, S. Q., Tang, Y. M., and Yin, Y. S., 2006, "Effects of Nanoparticle Clustering and Alignment On Thermal Conductivities of Fe3O4 Aqueous Nanofluids," Appl. Phys. Lett., **89**(2), p. 023123.
[73] Zhu, H. T., Zhang, C. Y., Tang, Y. M., and Wang, J. X., 2007, "Novel Synthesis and Thermal Conductivity of CuO Nanofluid," J. Phys. Chem. C, **111**(4), pp. 1646–1650.
[74] Fricke, H., 1924, "A Mathematical Treatment of the Electric Conductivity and Capacity of Disperse Systems: I. The Electric Conductivity of a Suspension of Homogeneous Spheroids," Phys. Rev., **24**, pp. 575–587.
[75] Nan, C. W., 1993, "Physics of Inhomogeneous Inorganic Materials," Prog. Mater. Sci., **37**(1), pp. 1–116.
[76] Nan, C. W., Birringer, R., Clarke, D. R., and Gleiter, H., 1997, "Effective Thermal Conductivity of Particulate Composites With Interfacial Thermal Resistance," J. Appl. Phys., **81**(10), pp. 6692–6699.
[77] Prasher, R., Evans, W., Meakin, P., Fish, J., Phelan, P., and Keblinski, P., 2006, "Effect of Aggregation on Thermal Conduction in Colloidal Nanofluids," Appl. Phys. Lett., **89**, p. 143119.
[78] Gao, L., Zhou, X., and Ding, Y., 2007, "Effective Thermal and Electrical Conductivity of Carbon Nanotube Composites," Chem. Phys. Lett., **434**, pp. 297–300.
[79] Nan, C. W., Shi, Z., and Lin, Y., 2003, "A Simple Model for Thermal Conductivity of Carbon Nanotube-Based Composites," Chem. Phys. Lett., **375**, pp. 666–669.
[80] Patel, H. E., Anoop, K. B., Sundararajan, T., and Das, S. K., 2008, "Model for Thermal Conductivity of CNT-Nanofluids," Bull. Mater. Sci., **31**(3), pp. 387–390.
[81] Xue, Q. Z., 2005, "Model for Thermal Conductivity of Carbon Nanotube-Based Composites," Physica B, **368**(1–4), pp. 302–307.
[82] Xue, Q. Z., 2006, "Model for the Effective Thermal Conductivity of Carbon Nanotube Composites," Nanotechnology, **17**, pp. 1655–1660.
[83] Zhou, X. F., and Gao, L., 2006, "Effective Thermal Conductivity in Nanofluids of Nonspherical Particles With Interfacial Thermal Resistance: Differential Effective Medium Theory," J. Appl. Phys., **100**, p. 024913.
[84] Furth, R., 1956, *Investigations on the Theory of the Brownian Movement by Albert Einstein*, Dover, New York.
[85] Prasher, R., 2005, "Thermal Conductivity of Nanoscale Colloidal Solutions (Nanofluids)," Phys. Rev. Lett., **94**, p. 025901.
[86] Eapen, J., Rusconi, R., Piazza, R., and Yip, S., 2010, "The Classical Nature of Thermal Conduction in Nanofluids," ASME J. Heat Transfer, **132**(10), p. 102402.
[87] Evans, W., Fish, J., and Keblinski, P., 2006, "Role of Brownian Motion Hydrodynamics on Nanofluid Thermal Conductivity," Appl. Phys. Lett., **88**(9), p. 093116.
[88] Piazza, R., 2004, "'Thermal Forces': Colloids in Temperature Gradients," J. Phys.: Condens. Matter, **16**(38), pp. S4195–S4211.
[89] Gupte, S. K., Advani, S. G., and Huq, P., 1995, "Role of Micro-Convection Due to Non-Affine Motion of Particles in a Mono-Disperse Suspension," Int. J. Heat Mass Transfer, **38**(16), pp. 2945–2958.
[90] Leal, L. G., 1973, "On the Effective Conductivity of a Dilute Suspension of Spherical Drops in the Limit of Low Particle Peclet Number," Chem. Eng. Commun., **1**(1), pp. 21–31.
[91] Keblinski, P., and Thomin, J., 2006, "Hydrodynamic Field Around a Brownian Particle," Phys. Rev. E, **73**, p. 010502.
[92] Kuwabara, S., 1959, "The Forces Experienced by Randomly Distributed Parallel Circular Cylinders or Spheres in a Viscous Flow at Small Reynolds Numbers," J. Phys. Soc. Jpn., **14**, pp. 527–532.
[93] Jung, J. Y., and Yoo, J. Y., 2009, "Thermal Conductivity Enhancement of Nanofluids in Conjunction With Electrical Double Layer (EDL)," Int. J. Heat Mass Transfer, **52**, pp. 525–528.
[94] Domingues, G., Volz, S., Joulain, K., and Greffet, J. J., 2005, "Heat Transfer Between Two Nanoparticles Through Near Field Interaction," Phys. Rev. Lett., **94**(8), p. 085901.
[95] Ben-Abdallah, P., 2006, "Heat Transfer Through Near-Field Interactions in Nanofluids," Appl. Phys. Lett., **89**(11), p. 113117.
[96] Vadasz, J. J., Govender, S., and Vadasz, P., 2005, "Heat Transfer Enhancement in Nano-Fluids Suspensions: Possible Mechanisms and Explanations," Int. J. Heat Mass Transfer, **48**, pp. 2673–2683.
[97] Eapen, J., Li, J., and Yip, S., 2007, "Mechanism of Thermal Transport in Dilute Nanocolloids," Phys. Rev. Lett., **98**, p. 028302.
[98] Tzou, D. Y., 1997, *Macro- to Microscale Heat Transfer: The Lagging Behavior*, Taylor & Francis, Washington, DC.
[99] Wang, L. Q., Zhou, X. S., and Wei, X. H., 2008, *Heat Conduction: Mathematical Models and Analytical Solutions*, Springer-Verlag, Heidelberg.
[100] Buongiorno, J., Venerus, D. C., Prabhat, N., McKrell, T., Townsend, J., Christianson, R., Tolmachev, Y. V., Keblinski, P., Hu, L. W., Alvarado, J. L., Bang, I. C., Bishnoi, S. W., Bonetti, M., Botz, F., Cecere, A., Chang, Y., Chen, G., Chen, H., Chung, S. J., Chyu, M. K., Das, S. K., di Paola, R., Ding, Y., Dubois, F., Dzido, G., Eapen, J., Escher, W., Funfschilling, D., Galand, Q., Gao, J., Gharagozloo, P. E., Goodson, K. E., Gutierrez, J. G., Hong, H., Horton, M., Hwang, K. S., Iorio, C. S., Jang, S. P., Jarzebski, A. B., Jiang, Y., Jin, L., Kabelac, S., Kamath, A., Kedzierski, M. A., Kieng, L. G., Kim, C., Kim, J. H., Kim, S., Lee, S. H., Leong, K. C., Manna, I., Michel, B., Ni, R., Patel, H. E., Philip, J., Poulikakos, D., Reynaud, C., Savino, R., Singh, P. K., Song, P., Sundararajan, T., Timofeeva, E., Tritcak, T., Turanov, A. N., van Vaerenbergh, S., Wen, D., Witharana, S., Yang, C., Yeh, W. H., Zhao, X. Z.,

and Zhou, S. Q., 2009, "A Benchmark Study on the Thermal Conductivity of Nanofluids," J. Appl. Phys., **106**, p. 094312.
[101] Kang, H. U., Kim, S. H., and Oh, J. M., 2006, "Estimation Of Thermal Conductivity of Nanofluid Using Experimental Effective Particle Volume," Exp. Heat Transfer, **19**, pp. 181–191.
[102] Jana, S., Salehi-Khojin, A., and Zhong, W. H., 2007, "Enhancement of Fluid Thermal Conductivity by the Addition of Single and Hybrid Nano-Additives," Thermochim. Acta, **462**, pp. 45–55.
[103] Shaikh, S., Lafdi, K., and Ponnappan, R., 2007, "Thermal Conductivity Improvement in Carbon Nanoparticle Doped PAO-Oil," J. Appl. Phys., **101**, p. 064302.
[104] Wiener, O., 1912, "Die Theorie des Mischkörpers für das Feld der stationaren Strömung. Erste Abhandlung: Die Mittel wert sätze fur Kraft, Polarisation und Energie," Abh. Math.-Phys. Kl. Königl. *Sächs*. Ges., **32**, pp. 509–604.
[105] Nielsen, L. E., 1978, *Predicting the Properties of Mixtures: Mixture Rules in Science and Engineering*, Dekker, New York.
[106] Bottcher, C. J. F., 1945, "The Dielectric Constant of Crystalline Powders," Recueil des travaux chimiques des Pays-Bas, **64**, pp. 47–51.
[107] Bruggeman, D. A. G., 1935, "Berechnung verschiedener physikalischer Konstanten von heterogenen Substanzen, I. Dielektrizitatskonstanten und Leitfahigkeiten der Mischkorper aus isotropen Substanzen," Ann. Phys., **416**, pp. 636–664.
[108] Hashin, Z., and Shtrikman, S., 1962, "A Variational Approach to the Theory of the Effective Magnetic Permeability of Multiphase Materials," J. Appl. Phys., **33**(10), pp. 3125–3131.
[109] Kwak, K., and Kim, C., 2005, "Viscosity and Thermal Conductivity of Copper Oxide Nanofluid Dispersed in Ethylene Glycol," Korea-Aust. Rheol. J., **17**(2), pp. 35–40.
[110] Wen, D. S., and Ding, Y. L., 2004, "Experimental Investigation Into Convective Heat Transfer of Nanofluids at the Entrance Region Under Laminar Flow Conditions," Int. J. Heat Mass Transfer, **47**(24), pp. 5181–5188.
[111] Zhang, X., Gu, H., and Fujii, M., 2006, "Experimental Study on the Effective Thermal Conductivity and Thermal Diffusivity of Nanofluids," Int. J. Thermophys., **27**(2), pp. 569–580.
[112] Yu, W., and Choi, S. U. S., 2003, "The Role of Interfacial Layers in the Enhanced Thermal Conductivity of Nanofluids: A Renovated Maxwell Model," J. Nanopart. Res., **5**, pp. 167–171.
[113] Leong, K. C., Yang, C., and Murshed, S. M. S., 2006, "A Model for the Thermal Conductivity of Nanofluids—The Effect of Interfacial Layer," J. Nanopart. Res., **8**(2), pp. 245–254.
[114] Murshed, S. M. S., Leong, K. C., and Yang, C., 2009, "A Combined Model for the Effective Thermal Conductivity of Nanofluids," Appl. Therm. Eng., **29**, pp. 2477–2483.
[115] Wang, B. X., Zhou, L. P., and Peng, X. F., 2003, "A Fractal Model for Predicting the Effective Thermal Conductivity of Liquid With Suspension of Nanoparticles," Int. J. Heat Mass Transfer, **46**, pp. 2665–2672.
[116] Xue, Q., and Xu, W. M., 2005, "A Model of Thermal Conductivity of Nanofluids With Interfacial Shells," Mater. Chem. Phys., **90**(2–3), pp. 298–301.
[117] Yu, W., and Choi, S. U. S., 2004, "The Role of Interfacial Layers in the Enhanced Thermal Conductivity of Nanofluids: A Renovated Hamilton-Crosser Model," J. Nanopart. Res., **6**, pp. 355–361.
[118] Ren, Y., Xie, H., and Cai, A., 2005, "Effective Thermal Conductivity of Nanofluids Containing Spherical Nanoparticles," J. Phys. D, **38**(21), pp. 3958–3961.
[119] Xie, H. Q., Fujii, M., and Zhang, X., 2005, "Effect of Interfacial Nanolayer on the Effective Thermal Conductivity of Nanoparticle-Fluid Mixture," Int. J. Heat Mass Transfer, **48**(14), pp. 2926–2932.
[120] Xuan, Y. M., Li, Q., and Hu, W. F., 2003, "Aggregation Structure and Thermal Conductivity of Nanofluids," AIChE J., **49**(4), pp. 1038–1043.
[121] Xuan, Y., and Li, Q., 2000, "Heat Transfer Enhancement of Nanofluids," Int. J. Heat Fluid Flow, **21**(1), pp. 58–64.
[122] Jang, S. P., and Choi, S. U. S., 2004, "Role of Brownian Motion in the Enhanced Thermal Conductivity of Nanofluids," Appl. Phys. Lett., **84**(21), pp. 4316–4318.
[123] Jang, S. P., and Choi, S. U. S., 2007, "Effects of Various Parameters on Nanofluid Thermal Conductivity," ASME J. Heat Transfer, **129**(5), pp. 617–623.
[124] Chen, G., 1996, "Nonlocal and Nonequilibrium Heat Conduction in the Vicinity of Nanoparticles," ASME J. Heat Transfer, **118**(3), pp. 539–545.
[125] Kapitza, P. L., 1941, "The Study of Heat Transfer in Helium II," J. Phys. (Moscow), **4**, pp. 181–210.
[126] Prasher, R., Bhattacharya, P., and Phelan, P. E., 2006, "Brownian-Motion-Based Convective-Conductive Model for the Effective Thermal Conductivity of Nanofluids," ASME J. Heat Transfer, **128**(6), pp. 588–595.
[127] Koo, J., and Kleinstreuer, C., 2004, "A New Thermal Conductivity Model for Nanofluids," J. Nanopart. Res., **6**, pp. 577–588.
[128] Kumar, D. H., Patel, H. E., Kumar, V. R. R., Sundararajan, T., Pradeep, T., and Das, S. K., 2004, "Model for Heat Conduction in Nanofluids," Phys. Rev. Lett., **93**(14), p. 144301.
[129] Xu, J., Yu, B., Zhou, M., and Xu, P., 2006, "A New Model for Heat Conduction of Nanofluids Based on Fractal Distributions of Nanoparticles," J. Phys. D, **39**, pp. 4486–4490.
[130] Nan, C. W., Liu, G., Lin, Y., and Li, M., 2004, "Interface Effect on Thermal Conductivity of Carbon Nanotube Composites," Appl. Phys. Lett., **85**(16), pp. 3549–3551.
[131] Prasher, R., Phelan, P. E., and Bhattacharya, P., 2006, "Effect of Aggregation Kinetics on the Thermal Conductivity of Nanoscale Colloidal Solutions (Nanofluids)," Nano Lett., **6**(7), pp. 1529–1534.
[132] Evans, W., Prasher, R., Fish, J., Meakin, P., Phelan, P., and Keblinski, P., 2008, "Effect of Aggregation and Interfacial Thermal Resistance on Thermal Conductivity of Nanocomposites and Colloidal Nanofluids," Int. J. Heat Mass Transfer, **51**, pp. 1431–1438.
[133] Wang, L. Q., and Fan, J., 2010, "Nanofluids Research: Key issues," Nanoscale Res. Lett., **5**, pp. 1241–1252.
[134] Whitaker, S., 1999, *The Method of Volume Averaging*, Kluwer Academic, Dordrecht.
[135] Wang, L. Q., 2000, "Flows Through Porous Media: A Theoretical Development at Macroscale," Transp. Porous Media, **39**, pp. 1–24.
[136] Wang, L. Q., Xu, M. T., and Wei, X. H., 2008, "Multiscale Theorems," Adv. Chem. Eng., **34**, pp. 175–468.
[137] Wang, L. Q., and Wei, X., 2008, "Equivalence Between Dual-Phase-Lagging and Two-Phase-System Heat Conduction Processes," Int. J. Heat Mass Transfer, **51**, pp. 1751–1756.
[138] Quintard, M., and Whitaker, S., 2000, "Theoretical Analysis of Transport in Porous Media," *Handbook of Heat Transfer in Porous Media*, K. Vafai, ed., Dekker, New York, pp. 1–52.
[139] Xu, M. T., and Wang, L. Q., 2002, "Thermal Oscillation and Resonance in Dual-Phase-Lagging Heat Conduction," Int. Commun. Heat Mass Transfer, **45**, pp. 1055–1061.
[140] Fan, J., and Wang, L. Q., 2010, "Microstructural Effects on Macroscale Thermal Properties in Nanofluids," NANO, **5**(2), pp. 117–125.
[141] Fan, J., and Wang, L. Q., 2010, "Effective Thermal Conductivity of Nanofluids: the Effects of Microstructure," J. Phys. D: Appl. Phys., **43**, p. 165501.
[142] Fan, J., and Wang, L. Q., 2010, "Is Classical Energy Equation Adequate for Convective Heat Transfer in Nanofluids?," Adv. Mech. Eng., **2010**, p. 719406.